Correlation between DSC Curves and Isobaric State Diagrams. 1. Calculation of DSC Curves from Isobaric State Diagrams

Andreas Müller and Werner Borchard*

Angewandte Physikalische Chemie, Gerhard-Mercator-Universität Duisburg, Lotharstrasse 1, D-47048 Duisburg, Germany

Received: November 13, 1996; In Final Form: March 4, 1997[⊗]

The computation of isobaric DSC curves of binary mixtures from a known phase diagram is discussed. Based on the first law of thermodynamics, universal formulas are derived that allow us to calculate the course of the specific heat capacity as a function of temperature during a transition and, additionally, the respective base line. Despite being applied to the transition of fusion in our case, all relations are equally well applicable to any other transition such as sublimation and evaporation and also to mixing−demixing phenomena. They only require the knowledge of the equilibrium curves of the phase diagram (i.e. liquidus, solidus, and solvus curves) indicating the compositions of the coexisting phases at the prevailing temperatures. As invariant transitions quite often appear in many phase diagrams, the eutectic transition and the peritectic transition of fusion are treated quantitatively, leading to the so-called "Tammann's triangle" that characterizes the concentration-dependence of the enthalpy of transition. The calculated DSC curves prove to be coincident for the most part with the experimental data of the binary model system used, consisting of *n*-hexane (*n*-C_6H_{14}) and *n*-dodecane (*n*-$C_{12}H_{26}$). These results are likely to be improved by taking account of the so-called "smearing effect" of the DSC caused by processes of heat transfer during a DSC scan, which will be looked at in parts 2 and 3 of this series.

1. Introduction

According to Ehrenfest's terminology, phase transitions of pure substances (single-component systems), such as fusion, evaporation, and sublimation, are of first order, showing a discontinuity in enthalpy at the transition point.[1,2] The derivative thereof, the $\tilde{c}_P(T)$ curve, should therefore show a mathematical singularity, corresponding to an infinitely sharp transition. Unlike one-component systems, phase transitions of mixtures, i.e. systems containing at least two components, are not discontinuous in the first two derivatives of the Gibbs function. If, for example, we single out a transition of fusion of a binary system, the $\tilde{c}_P(T)$ curves are observed to be of the so-called λ-type in phenomenological terms, bearing a strong resemblance to a second-order transition of a pure substance.[3]

The goal of the present series of papers is to correlate isobaric DSC curves with isobaric state diagrams quantitatively.[4−7] State diagrams, also termed phase diagrams, are plots of transition temperatures of a mixture against temperature. They characterize, for instance, start and end temperatures of a transition for a certain composition, or conversely, they indicate the compositions of coexisting phases at a fixed temperature. DSC curves, obtained by means of differential scanning calorimetry (DSC), are records of specific heat capacities in dependence upon temperature, $\tilde{c}_P(T)$, and facilitate the characterization of almost every thermodynamic transition, always supposing, however, the transition is complete within the performance of the DSC scan. (Here, we assume that the specific heat capacity as a function of temperature, $\tilde{c}_P(T)$, is proportional to the heat flow recorded in dependence on time, $\dot{Q}(t)$, during a DSC scan. As we shall see in part 2 of this series, this proportionality holds satisfactorily in particular cases only.[4]) Proceeding on the assumption that both the initial state and the final state of this transition are distinctly represented by a finite number of variables (temperature, enthalpy, composition, etc.) so that internal equilibrium is established for the two states, the respective enthalpy of transition is independent of the pathway by which the final state has been reached. It is thus irrelevant that mostly the equilibrium state is slightly omitted by the intermediate states traversed during a DSC measurement. From the same reason, however, it is thoroughly difficult to determine heat capacities by this (dynamic) method inasmuch as those represent quantities related to the equilibrium state.[4]

Indeed, experimental transition peaks of pure substances (single-component systems) do not exhibit any singularity, as anticipated in thermodynamic terms, but are somewhat broadened out to a certain temperature range, which is a consequence of the experiment itself: Due to a limited (finite) heat flow in the DSC apparatus, a time delay is observed customarily called "smearing".[8] By the same token, λ-transitions which are already liable to a fusion *interval* are smeared, too. Note, smearing of transition peaks accounts for most of the difficulty in establishing accurate heat capacities by means of DSC.

The present part of this series focuses on computing the isobaric $\tilde{c}_P(T)$ courses of λ-transitions of fusion of a binary mixture from the underlying binary melting point or phase diagram, such as sketched in Figure 1. As invariant eutectic transitions precede λ-transitions quite frequently (actually if a complete solid solubility is not present), we shall also turn our attention to a thermodynamic treatment of the invariant eutectic transition of fusion. To complete the picture, the (quite rare) invariant peritectic transition of fusion will also be treated briefly. Throughout this paper we shall tacitly be assuming genuine intermediate equilibrium states despite being marginally failed in fact. As we shall see, however, the exact thermodynamic expressions of the $\tilde{c}_P(T)$ curves may serve, in first approximation, as a quantitative approach to real DSC curves providing "ideal" (i.e. nonsmeared) traces of DSC curves. This will be shown using *n*-hexane/*n*-dodecane as a binary model system. In connection with this, it must be emphasized that

* To whom correspondence should be addressed.

[⊗] Abstract published in *Advance ACS Abstracts,* April 15, 1997.

S1089-5647(96)03781-9 CCC: $14.00

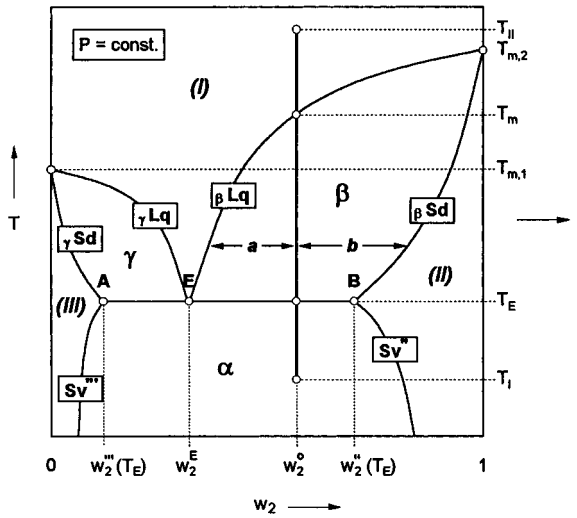

Figure 1. Binary eutectic phase diagram depicting temperature T versus mass fraction w_2 of component 2 with limited miscibility in the solid state. Vertical solid line (bold): route of a DSC scan through the phase diagram. α, β, and γ: state indices; $'$, $''$, $'''$: phase indices; $_\gamma$**Lq**, $_\beta$**Lq**: liquidus curves. $_\gamma$**Sd**, $_\beta$**Sd**: solidus curves. **Sv**$'''$, **Sv**$''$: solvus curves (see text).

we shall restrict the following discussion to considering DSC curves exclusively obtained by heating (i.e. curves with endothermic events) because practical cooling rates mostly provide conditions that do not allow a crystal to establish equilibrium states—even during the lowest experimentally measurable rates—due to nucleation and growth and due to extremely slow diffusion rates in solids.[9]

Inspection of experimental eutectic transition peaks of fusion will reveal that their widths are markedly governed by the initial composition of the test sample. This dependence will be looked at in the second part of this series[4] by making use of O'Neill's model[10] for sharply melting compounds that will be applied to the invariant eutectic transition. Aside from doing this, we shall shortly digress to work out the interrelation between the heat flow—which is, in effect, recorded during a DSC scan in dependence on time—and the specific heat capacity, usually given as a function of temperature. As we shall find out, this proportionality is only satisfied under certain circumstances: small mass of the test sample, low scanning speed, good thermal conductors as test sample.

The third part of this series[5] is devoted to simulating "real" (smeared) DSC curves. Starting out from the melting peaks of pure compounds that will be traced by a Gaussian distribution, we shall be simulating the course of real DSC curves of λ-transitions or rather the respective process of fusion during λ-transitions as if it were made up of multiple sharp fusion processes at different temperatures, the underlying fusion process notwithstanding. The eutectic fusion peaks will be traced by one Gaussian curve only, whose width will be fitted pursuant to the concentration-dependence derived in the second part of the series.[4]

Part 4 of this series[6] will deal with the construction of approximated base lines. Inasmuch as heat capacities cannot be determined with sufficient accuracy using DSC (resulting in DSC curves being incompatible with the base lines calculated from the relations of the present part), a novel base line method will be developed that establishes base lines independently of the experimentally obtained values of heat capacity. This base line method will, in turn, be required in the last part of this series[7] in order to do, so to speak, the "reverse step" of our considerations here, i.e. to recalculate an isobaric state diagram from one single DSC curve. As we shall see finally, this is quite possible in certain cases.

2. Thermodynamic Considerations

Let us first look at the schematical plot of a phase diagram shown in Figure 1 in order to see more clearly what we intend to do. Figure 1 depicts a eutectic phase diagram with a partial miscibility of the solid components. The reason we have chosen this sort of state digram was that this particular type comprehends almost any of the so-called Roozeboom phase diagrams of solid solution systems,[11,12] such as unlimited solubility in the solid state with or without an azeotropic point, respectively, limited solubility with a peritectic or a eutectic point, and finally—once the miscibility gap within the solid state is entirely extended to the ordinates—no solubility in the solid state combined with a eutectic point.

Figure 1 contains six regions, each of which is enclosed by a certain number of equilibrium curves such as the liquidus curves ($_\beta$**Lq**, $_\gamma$**Lq**) or the solidus curves ($_\beta$**Sd**, $_\gamma$**Sd**) representing the composition of the melt ***(I)*** and the mixed crystal ***(II)*** or ***(III)*** concerning the liquid−solid equilibria β or γ, respectively, or the solvus curves **Sv**$''$ and **Sv**$'''$ representing the composition of the solid solution ***(II)*** or ***(III)*** but in the solid−solid equilibrium α. Above the liquidus curves a single-phase region of the homogeneous liquid mixture ***(I)*** designated by the superscript ($'$) is observed. Beneath the eutectic temperature, T_E, within the mass fractions ranging from $w_2'''$to w_2'', a two-phase region is formed comprising two coexisting mixed crystals ***(II)*** and ***(III)***. This state will be indicated by the index α.

At intermediate temperatures, that is, below the liquidus curves but above the solvus curves, two homogeneous and two heterogeneous regions appear, depending on the overall or initial composition w_2°, which is given in the mass fraction scale of component 2. If w_2° ranges from 0 to w_2'''or from w_2'' to 1, the homogeneous or single-phase region, enclosed by the solidus curve, the solvus curve, and the ordinate, will be established. The other two heterogeneous phases, separated from the homogeneous regions by the liquidus and solidus curves represent the solid−liquid equilibria γ and β of the melt ***(I)*** and a mixed crystal ***(III)*** or ***(II)***, respectively.

The eutectic mixture is obtained if a liquid mixture ***(I)*** with a composition ranging from $w_2'''$to w_2'' is cooled down to the eutectic temperature T_E. First, on passing the liquidus curve, a mixed crystal begins separating out, actually as long as the composition of the liquid mixture has not approached that of the eutectic point **E**, while that of the mixed crystal alters continuously toward w_2'''or w_2''. Hence, the relative amounts of both the liquid mixture and the mixed crystal change following the lever rule provided, however, that equilibrium states are attained by all intermediates traversed. (Let us shortly explain what the lever rules states: following simple mass conservation considerations, the amounts of two coexisting phases (e.g. the phase mass ratio between melt and crystal) are inversely proportional to their "distances" from the overall composition of the system (see ratio b : a at an arbitrary temperature T in Figure 1).[9]) Once the eutectic temperature T_E is reached, the last remaining liquid ***(I)***, at present with eutectic composition w_2^E, coexists with the two solid phases ***(III)*** and ***(II)***, as long as the liquid is not completely transformed to the solid phases yet.

Figure 1 further contains a single route straight through the state diagram, being traced in the course of a DSC measurement. Starting at temperature T_I that represents the onset of measurement and passing through the invariant transition at T_E, the end of fusion, T_m, will be approached finally. Once temperature T_{II} is eventually reached, the DSC scan will be terminated. For

this reason the calculation of the DSC curve from the underlying track of measurement requires distinguishing between four ranges: first, there is that prior to eutectic melting, afterward the infinitely sharp eutectic transition, followed by the fusion of the mixed crystal (λ-transition), and finally the range of the melt. Inasmuch as the aforementioned track—or rather the initial composition w_2°—has been chosen so that both the eutectic transition and the fusion of the mixed crystal are involved, one is equally capable of calculating DSC curves of any binary mixture showing a complete solid solubility, for instance $w_2^\circ \leq w_2'''$ or $w_2^\circ \geq w_2''$. In this case, the eutectic transition is absent, and merely three ranges are to be regarded: the range of the homogeneous solid solution prior to fusion (crystal ***(II)*** or ***(III)***), the λ-transition of fusion, and the range of the melt above the melting temperture T_m of the binary test sample.

Before we now turn to a quantitative description of these four ranges in question, let us shortly survey the following six sections. Sections 2.1 to 2.3 will be dealing with invariant transitions, the first of which is devoted to a rigorous thermodynamic treatment of the eutectic transition of fusion. As we shall see, the resulting final expressions may be understood to be a quantitative approach to the so-called "Tammann's triangle".[13] This will further be discussed in section 2.2 and some of the consequences arising out of that. Subsequently in section 2.3, the invariant peritectic transition of fusion will be treated in broad outline.

In section 2.4, we shall be dealing with a thermodynamic description of the λ-transition that runs from the eutectic temperature T_E to the melting point T_m of the mixture (see Figure 1). In doing so, we shall realize the advantage of the formalism used. It enables us to characterize the real phase behavior of the system on the basis of separated variables, being split up into thermal properties of the pure compounds, on one hand, and mixing quantities, on the other hand. Finally, in sections 2.5 and 2.6, we shall consider the temperature range of the crystal prior to fusion (first range) and that of the melt above T_m (fourth range).

2.1. Eutectic Enthalpy of Fusion. In this section the eutectic transition will first be considered for an overall concentration $w_2^E \leq w_2^\circ \leq w_2''$, i.e. for the equilibrium states in the regions β and α at $T = T_E$, so that the specific eutectic enthalpy of fusion $\Delta\tilde{H}_E$ should arise from the difference between ${}_\beta\tilde{H}_{T_E}$ and ${}_\alpha\tilde{H}_{T_E}$, indicating the overall specific enthalpies of the states β and α at $T = T_E$:

$$\Delta\tilde{H}_E = {}_\beta\tilde{H}_{T_E} - {}_\alpha\tilde{H}_{T_E} \tag{1a}$$

As we shall see, our first approach to a quantitative description of the specific eutectic enthalpy pursuant to eq 1a will lead to an expression being inconvenient to manage. This is mainly due to the fact that ${}_\beta\tilde{H}_{T_E}$ and ${}_\alpha\tilde{H}_{T_E}$ pertain to different concentration ranges so that hypothetic quantities will appear that are experimentally not accessible in a direct way. To circumvent this difficulty, we shall introduce enthalpies of transfer that serve to regard the eutectic transition as if it were made up of a certain number of hypothetical steps. Finally, the eutectic transition will also be applied to the other concentration range ($w_2''' \leq w_2^\circ \leq w_2^E$) concerning the equilibria γ and α. In this case, $\Delta\tilde{H}_E$ is given by the relation

$$\Delta\tilde{H}_E = {}_\gamma\tilde{H}_{T_E} - {}_\alpha\tilde{H}_{T_E} \tag{1b}$$

where ${}_\gamma\tilde{H}_{T_E}$ designates the overall enthalpy of state γ at the eutectic temperature (see Figure 1). Note, the reader may shorten the study of this section by directly turning from here to the final expressions for $\Delta\tilde{H}_E$ in eqs 34a and 34b. To this end, all principal symbols of quantities used have been listed in the glossary appended to this paper.

According to Figure 1, state β consists of two phases, namely the liquid phase ***(I)*** designated by index ($'$) and the mixed crystal ***(II)*** bearing the index ($''$). Let ${}_\beta H$, ${}_\beta H'$, and ${}_\beta H''$ be the enthalpy of the two-phase system, the enthalpy of phase ($'$) and that of phase ($''$) referred to state β. Thus the enthalpy of this state reads

$${}_\beta H = {}_\beta H' + {}_\beta H'' \tag{2a}$$

This equation holds in the total temperature range in which the two phases in question are coexistent. Introducing the specific enthalpies ${}_\beta\tilde{H}'$ and ${}_\beta\tilde{H}''$ affords

$${}_\beta H' = {}_\beta\tilde{H}'\,{}_\beta m' \quad \text{and} \quad {}_\beta H'' = {}_\beta\tilde{H}''\,{}_\beta m'' \tag{3a}$$

where ${}_\beta m'$ and ${}_\beta m''$ are the masses of phases ($'$) and ($''$). Application of the relation of Euler leads to the identities

$${}_\beta\tilde{H}' = \sum_i {}_\beta w_i'\,{}_\beta\tilde{H}_i' \quad \text{and} \quad {}_\beta\tilde{H}'' = \sum_i {}_\beta w_i''\,{}_\beta\tilde{H}_i'' \tag{4a}$$

Here, ${}_\beta\tilde{H}_i'$ and ${}_\beta\tilde{H}_i''$ are the partial specific enthalpies of component i ($i = 1, 2$) in phase ($'$) or phase ($''$) referred to state β; ${}_\beta w_i'$ and ${}_\beta w_i''$ defined by ${}_\beta w_i' = {}_\beta m_i'/{}_\beta m'$ and ${}_\beta w_i'' = {}_\beta m_i''/{}_\beta m''$ denote the corresponding mass fractions of component i in the coexisting phases ($'$) and ($''$) whereby ${}_\beta m_i'$ and ${}_\beta m_i''$ are the masses of component i in the liquid or solid phase. Combination of eqs 2a−4a yields the enthalpy of the two-phase system at the eutectic temperature:

$${}_\beta H_{T_E} = [{}_\beta m'({}_\beta w_{1\beta}'\tilde{H}_1' + {}_\beta w_{2\beta}'\tilde{H}_2') + {}_\beta m''({}_\beta w_{1\beta}''\tilde{H}_1'' + {}_\beta w_{2\beta}''\tilde{H}_2'')]_{T=T_E} \tag{5a}$$

Since the eutectic transition is considered to be infinitely sharp, the compositions of the three coexisting phases ***(III)***, ***(II)***, and ***(E)*** present at the eutectic temperature should not change. It is thus irrelevant to the mass fractions which states are actually underlying, for instance ${}_\beta w_i'' = {}_\alpha w_i'' \equiv w_i''$, so that we may abolish the indication of states from now on with regard to the mass fractions. Due to clarity, we further replace all superscripts ($'$) by (^{E}), such as $w_i' = w_i^E$. It is worth noting here that the enthalpies occurring in eq 5a are fixed quantities inasmuch as pressure (P = const), temperature (T_E), and compositions, such as $w_2'''(T_E)$, w_2^E, and $w_2''(T_E)$, remain constant (see Figure 1).

Using the mass conservation for the phase equilibria corresponding to the states α and β, and the mass conservation of component i in all coexisting phases, we obtain

$$m \equiv {}_\beta m = {}_\beta m^E + {}_\beta m'' \tag{6a}$$

and

$$m \equiv {}_\alpha m = {}_\alpha m'' + {}_\alpha m''' \tag{6b}$$

or, if component 2 is considered,

$${}_\beta m w_2^\circ = {}_\beta m^E w_2^E + {}_\beta m'' w_2'' \tag{7a}$$

and

$${}_\alpha m w_2^\circ = {}_\alpha m''' w_2''' + {}_\alpha m'' w_2'' \tag{7b}$$

where m, ${}_\beta m$, ${}_\alpha m$, ${}_\beta m^E$, ${}_\beta m''$, ${}_\alpha m''$, and ${}_\alpha m'''$ are the total masses belonging to the original state, to state α and β, respectively, and also to different phases (^{E}, $''$, and $'''$); w_2° is the overall or

initial composition of component 2 in the mass fraction scale defined by $w_2^\circ = m_2/m$, and w_2'', w_2''', w_2^E are understood to be the mass fractions of component 2 in the phases ($''$), ($'''$), and the liquid eutectic phases at the eutectic point **E** (see Figure 1). Additionally, every binary phase δ (with $\delta = ''$, $'''$, or ^{E}) must fulfill the condition

$$\sum_{i=1}^{2} w_i^\delta = 1 \tag{8}$$

Combination of eqs 6a and 7a results in

$$\frac{{}_\beta m^E}{m} = \frac{w_2'' - w_2^\circ}{w_2'' - w_2^E} \tag{9a}$$

and

$$\frac{{}_\beta m''}{m} = \frac{w_2^\circ - w_2^E}{w_2'' - w_2^E} \tag{10a}$$

while using eqs 6b and 7b yields

$$\frac{{}_\alpha m'''}{m} = \frac{w_2^\circ - w_2'''}{w_2'' - w_2'''} \tag{9b}$$

and

$$\frac{{}_\alpha m'''}{m} = \frac{w_2'' - w_2^\circ}{w_2'' - w_2'''} \tag{10b}$$

These relations are the lever rule in a little different form. (As opposed to the lever rule in its original form, eqs 9a−10b correspond to a mass ratio between a single phase and the total system *and not* between two coexisting phases.) By use of eqs 8, 9a, and 10a, and substituting phase index (^{E}) for ($'$), as mentioned above, eq 5a may now be condensed to

$${}_\beta\tilde{H}_{T_E} = \frac{w_2'' - w_2^\circ}{w_2'' - w_2^E}[(1 - w_2^E)_\beta\tilde{H}_1^E + w_{2\beta}^E\tilde{H}_2^E] + \frac{w_2^\circ - w_2^E}{w_2'' - w_2^E}[(1 - w_2'')_\beta\tilde{H}_1'' + w_{2\beta}''\tilde{H}_2'']_{T=T_E} \tag{11a}$$

where ${}_\beta\tilde{H}_{T_E} \equiv {}_\beta H_{T_E}/m$ designates the overall specific enthalpy of the final state β of the eutectic transition at the eutectic temperature; the terms in front of the square brackets represent the masses of the corresponding phases (^{E}) and ($''$) related to the total mass m. Equation 11a obtained comprises the sum of two terms of which the first one corresponds to the eutectic melt. The second term represents the remaining quantity, namely, the crystal ***(II)***, which will be fused in the course of the subsequent melting transition within the respective temperature range from $T = T_E$ to $T = T_m$ (see Figure 1).

Proceeding as before, the enthalpy of state α concerning the two-phase equilibrium between the two mixed crystals ***(II)*** and ***(III)*** is given by

$${}_\alpha H = {}_\alpha H'' + {}_\alpha H''' \tag{2b}$$

In analogy to eqs 3a and 4a we get

$${}_\alpha H'' = {}_\alpha\tilde{H}''\,{}_\alpha m'' \quad \text{and} \quad {}_\alpha H''' = {}_\alpha\tilde{H}'''\,{}_\alpha m''' \tag{3b}$$

and

$${}_\alpha\tilde{H}'' = \sum_i {}_\alpha w_i''\,{}_\alpha\tilde{H}_i'' \quad \text{and} \quad {}_\alpha\tilde{H}''' = \sum_i {}_\alpha w_i'''\,{}_\alpha\tilde{H}_i''' \tag{4b}$$

where ${}_\alpha H''$ or ${}_\alpha H'''$, and ${}_\alpha\tilde{H}_i''$ or ${}_\alpha\tilde{H}_i'''$ are the enthalpies of the mixed crystals in the phases ($''$) or ($'''$) and the partial specific enthalpies of component i ($i = 1, 2$) in the coexisting phases ($''$) or ($'''$), respectively; all quantities are related to the heterogeneous equilibrium characterized by state α. Substituting eqs 3b and 4b for ${}_\alpha H''$ and ${}_\alpha H'''$ in eq 2b and canceling the state index for the weight fractions (see above) gives

$${}_\alpha H_{T_E} = [{}_\alpha m''(w_{1\alpha}''\tilde{H}_1'' + w_{2\alpha}''\tilde{H}_2'') + {}_\alpha m'''(w_{1\alpha}'''\tilde{H}_1''' + w_{2\alpha}'''\tilde{H}_2''')]_{T=T_E} \tag{5b}$$

in which all quantities refer to the eutectic temperature ($T = T_E$). Using eqs 9b and 10b furnishes the analogous expression to eq 11a:

$${}_\alpha\tilde{H}_{T_E} = \frac{w_2^\circ - w_2'''}{w_2'' - w_2'''}[(1 - w_2'')_\alpha\tilde{H}_1'' + w_{2\alpha}''\tilde{H}_2'']_{T=T_E} + \frac{w_2'' - w_2^\circ}{w_2'' - w_2'''}[(1 - w_2''')_\alpha\tilde{H}_1''' + w_{2\alpha}'''\tilde{H}_2''']_{T=T_E} \tag{11b}$$

Consequently, the enthalpy change due to eutectic melting, $\Delta\tilde{H}_E$, can be achieved by combining eqs 11a with 11b pursuant to eq 1a. As, however, the quantities ${}_\alpha\tilde{H}_i'''$ and ${}_\beta\tilde{H}_i^E$ belong to different concentrations, w_2''' and w_2^E in fact, eq 11b proves to be inconvenient to manage. We shall thus show now how eq 11b can be related to other quantities experimentally available to avoid this difficulty. To this end, we proceed by considering the eutectic transition to occur by the following (hypothetical) steps. Starting out at the eutectic temperature T_E, where only the state α is assumed to exist, we increase temperature T_E to ($T_E + \delta T$) by an infinitely small temperature step δT, whereupon state β is established. This equilibrium, as stated above, is characterized by both a liquid quantity, ${}_\beta m^E$, and a crystalline quantity, ${}_\beta m''$, that will melt within the temperature range $T_E < T < T_m$. With regard to Figure 1 with the case $w_2^E \le w_2^\circ \le w_2''$ depicted therein, the entire mass ${}_\alpha m'''$ of the mixed crystal ***(III)*** and a certain amount Δm of crystal ***(II)*** undergo fusion in the course of the eutectic transition to give composition w_2^E; this proportion involved is also identical with mass ${}_\beta m^E$ at temperature ($T_E + \delta T$). Conversely, a certain amount of crystal ***(II)***, actually mass ${}_\alpha m''$ reduced by Δm, must remain solid during the eutectic fusion, equivalent to mass ${}_\beta m''$ at temperature ($T_E + \delta T$). Hence,

$${}_\alpha m'''_{T=T_E} + \Delta m \equiv {}_\beta m^E_{T=T_E+\delta T} \tag{12}$$

and

$${}_\alpha m''_{T=T_E} - \Delta m \equiv {}_\beta m''_{T=T_E+\delta T} \tag{13}$$

Owing to the conservation of the total mass m,

$$m \equiv {}_\alpha m'''_{T=T_E} + {}_\alpha m''_{T=T_E} = {}_\beta m^E_{T=T_E+\delta T} + {}_\beta m''_{T=T_E+\delta T} \tag{14}$$

and omitting the indication of temperature, Δm must be given by the expression

$$\Delta m \equiv {}_\alpha m'' - {}_\beta m'' = {}_\beta m^E - {}_\alpha m''' \tag{15}$$

that will result in

$$\frac{\Delta m}{m} = \frac{w_2'' - w_2^\circ}{w_2'' - w_2^E}\frac{w_2^E - w_2'''}{w_2'' - w_2'''} > 0 \qquad (16)$$

if eqs 9a and 10b, or eqs 9b and 10a, respectively, are taken. Note that Δm must be positive since $w_2''' < w_2^E < w_2''$ and $w_2^\circ < w_2''$. By use of eqs 4b and 15, eq 5b may be rewritten in the form

$${}_\alpha H_{T_E} = [{}_\alpha m''' {}_\alpha\tilde{H}''' + \Delta m {}_\alpha\tilde{H}'' + ({}_\alpha m'' - \Delta m){}_\alpha\tilde{H}'']_{T=T_E} \qquad (17)$$

Clearly, the first two terms are identical with the amount that will undergo the eutectic transition of fusion, while the third term is related to that of the crystal ***(II)*** that is still solid at $T = T_E + \delta T$. Since, however, $w_2'' \neq w_2^E$ and $w_2'' \neq w_2^E$, enthalpies of transfer[14] may now be introduced into ${}_\alpha\tilde{H}''$ and ${}_\alpha\tilde{H}'''$ in order to regard the isothermal eutectic melting procedure as an imaginary transfer of the entire crystal ***(III)*** from point **A** to **E** and of a part of crystal ***(II)***, actually Δm, from point **B** to **E** followed by a transfer of this eutectic mixture from temperature T_E (state α) to temperature $T_E + \delta T$ (state β) at point **E** (see Figure 1). Let $({}_\alpha\tilde{H}''' - {}_\alpha\tilde{H}^E) \equiv \Delta\tilde{H}_{III\to E}$ and $({}_\alpha\tilde{H}'' - {}_\alpha\tilde{H}^E) \equiv \Delta\tilde{H}_{II\to E}$ denote the enthalpies of transfer and let

$${}_\alpha\tilde{H}^E = (1 - w_2^E){}_\alpha\tilde{H}_1^E + w_{2\alpha}^E\tilde{H}_2^E \qquad (18)$$

be the enthalpy of those amounts just transferred from ***(III)*** to ***(E)*** and from ***(II)*** to ***(E)*** and related to the state α that will immediately be molten in the following "eutectic reaction" (see Figure 2). Replacing the first two terms in eq 17 by

$${}_\alpha m''' {}_\alpha\tilde{H}''' \equiv {}_\alpha m'''({}_\alpha\tilde{H}''' - {}_\alpha\tilde{H}^E) + {}_\alpha m''' {}_\alpha\tilde{H}^E \qquad (19)$$

and

$$\Delta m {}_\alpha\tilde{H}'' \equiv \Delta m({}_\alpha\tilde{H}'' - {}_\alpha\tilde{H}^E) + \Delta m {}_\alpha\tilde{H}^E \qquad (20)$$

eq 17 becomes

$${}_\alpha H_{T_E} = {}_\alpha m'''({}_\alpha\tilde{H}''' - {}_\alpha\tilde{H}^E) + \Delta m({}_\alpha\tilde{H}'' - {}_\alpha\tilde{H}^E) + ({}_\alpha m''' + \Delta m){}_\alpha\tilde{H}^E + ({}_\alpha m'' - \Delta m){}_\alpha\tilde{H}'' \qquad (21)$$

in which the first three terms represent that portion subject to fusion, and the last one corresponds to that portion of crystal ***(II)*** that is still solid at temperature $T = T_E + \delta T$. By using eqs 10b and 15, $({}_\alpha m''' + \Delta m)$ may be shown to be

$$({}_\alpha m''' + \Delta m) = m\frac{w_2'' - w_2^\circ}{w_2'' - w_2^E} \equiv {}_\beta m^E \qquad (22)$$

whereas $({}_\alpha m'' - \Delta m)$ arises from eqs 9b and 15,

$$({}_\alpha m'' - \Delta m) = m\frac{w_2^\circ - w_2^E}{w_2'' - w_2^E} \equiv {}_\beta m'' \qquad (23)$$

Substitution of eqs 10b, 16, 22, and 23 for ${}_\alpha m'''$, Δm, $({}_\alpha m''' + \Delta m)$, and $({}_\alpha m'' - \Delta m)$ in eq 21 and using the definition ${}_\alpha\tilde{H}_{T_E} \equiv {}_\alpha H_{T_E}/m$ gives

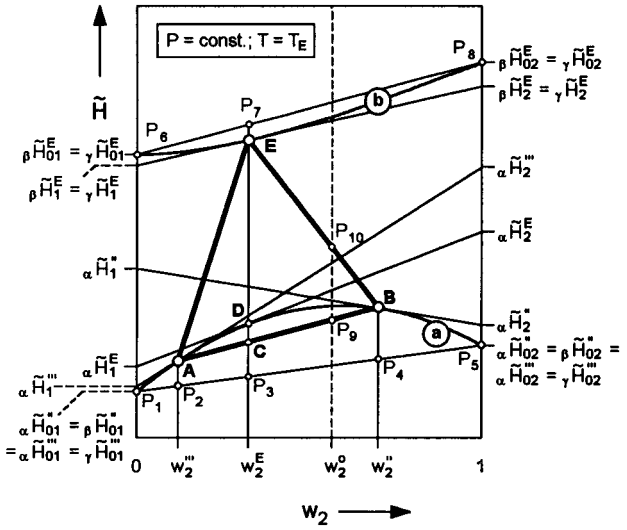

Figure 2. Geometrical relationship between the specific eutectic enthalpy of fusion, $\Delta\tilde{H}_E$, and the underlying specific enthalpies in an isobaric enthalpy−concentration diagram at the eutectic temperature. $\overline{P_1P_5}$ and curve a: ideal and real behavior of the solid phases. $\overline{P_6P_8}$ and curve b: ideal and real behavior of the liquid phase. The "Tammann's triangle" connecting points **A**, **E**, and **B** (bold line) reflects the invariant eutectic transition of the three coexisting phases (see text).

$${}_\alpha\tilde{H}_{T_E} = \left\{\frac{w_2'' - w_2^\circ}{w_2'' - w_2'''}({}_\alpha\tilde{H}''' - {}_\alpha\tilde{H}^E) + \frac{w_2'' - w_2^\circ}{w_2'' - w_2'''}\frac{w_2^E - w_2'''}{w_2'' - w_2^E}({}_\alpha\tilde{H}'' - {}_\alpha\tilde{H}^E) + \frac{w_2'' - w_2^\circ}{w_2'' - w_2^E}[(1 - w_2^E){}_\alpha\tilde{H}_1^E + w_{2\alpha}^E\tilde{H}_2^E] + \frac{w_2^\circ - w_2^E}{w_2'' - w_2^E}[(1 - w_2'){}_\alpha\tilde{H}_1'' + w_{2\alpha}''\tilde{H}_2'']\right\}_{T=T_E} \qquad (24)$$

which may be shown to be equivalent to eq 11b with $w_2'''$and w_2'' taken to be 0 and 1 for simplicity. Combination of eq 11a and eq 24 pursuant to eq 1a results in

$$\Delta\tilde{H}_E = \left\{\frac{w_2'' - w_2^\circ}{w_2'' - w_2^E}[(1 - w_2^E)({}_\beta\tilde{H}_1^E - {}_\alpha\tilde{H}_1^E) + w_2^E({}_\beta\tilde{H}_2^E - {}_\alpha\tilde{H}_2^E)] - \frac{w_2'' - w_2^\circ}{w_2'' - w_2'''}({}_\alpha\tilde{H}''' - {}_\alpha\tilde{H}^E) - \frac{w_2'' - w_2^\circ}{w_2'' - w_2'''}\frac{w_2^E - w_2'''}{w_2'' - w_2^E}({}_\alpha\tilde{H}'' - {}_\alpha\tilde{H}^E)\right\}_{T=T_E} \qquad (25)$$

Here, it must be observed that the contribution of the remaining crystal ***(II)*** disappears, namely, the quantity $({}_\alpha m'' - \Delta m)$ represented by the second term of eq 24, owing to ${}_\alpha\tilde{H}_1'' = {}_\beta\tilde{H}_1''$ and ${}_\alpha\tilde{H}_2'' = {}_\beta\tilde{H}_2''$. That is, despite being related to different states α and β, these quantities belong to the same solid phase ($''$). We now set about replacing the partial specific enthalpies and the enthalpies of transfer in eq 25 in terms of directly measurable quantities. Introducing the specific enthalpies of mixing, $\Delta_\epsilon\tilde{H}_{\epsilon mix}^\delta$, related to phase $\delta = ({}^E), (''), (''')$ and state $\epsilon = \alpha$ or β, respectively, we get

$$\Delta_\epsilon\tilde{H}_{mix}^\delta = (1 - w_2^\delta)({}_\epsilon\tilde{H}_1^\delta - {}_\epsilon\tilde{H}_{01}^\delta) + w_2^\delta({}_\epsilon\tilde{H}_2^\delta - {}_\epsilon\tilde{H}_{02}^\delta) \qquad (26)$$

where ${}_\epsilon\tilde{H}_{01}^\delta$ or ${}_\epsilon\tilde{H}_{02}^\delta$ denote the enthalpies of the pure compo-

nents 1 or 2 of the phase δ and the equilibrium ϵ, and ${}_\epsilon\tilde{H}_1^\delta$ or ${}_\epsilon\tilde{H}_2^\delta$ denotes the respective partial enthalpies (see Figure 2). Hence, the overall specific enthalpy of phase δ with respect to the equilibrium ϵ, ${}_\epsilon\tilde{H}^\delta$, reads

$$ {}_\epsilon\tilde{H}^\delta \equiv (1 - w_2^\delta)\,{}_\epsilon\tilde{H}_1^\delta + w_2^\delta\,{}_\epsilon\tilde{H}_2^\delta = (1 - w_2^\delta)\,{}_\epsilon\tilde{H}_{01}^\delta + w_2^\delta\,{}_\epsilon\tilde{H}_{02}^\delta + \Delta_\epsilon\tilde{H}_{\mathrm{mix}}^\delta \quad (27) $$

For notational convenience, we now set ${}_\alpha\tilde{H}_{0i} \equiv {}_\alpha\tilde{H}_{0i}^\delta$ with $i = 1, 2$ and $\delta = (^{\mathrm{E}})$, $('')$, $(''')$, and ${}_\beta\tilde{H}_{0i} \equiv {}_\beta\tilde{H}_{0i}^{\mathrm{E}}$ bearing in mind that ${}_\alpha\tilde{H}_{0i}$ and ${}_\beta\tilde{H}_{0i}$ belong to the crystalline state α or the liquid state β, respectively. According to eq 27, the first bracketed term in eq 25 may be expressed as

$$ [(1 - w_2^{\mathrm{E}})({}_\beta\tilde{H}_1^{\mathrm{E}} - {}_\alpha\tilde{H}_1^{\mathrm{E}}) + w_2^{\mathrm{E}}({}_\beta\tilde{H}_2^{\mathrm{E}} - {}_\alpha\tilde{H}_2^{\mathrm{E}})]_{T=T_{\mathrm{E}}} \equiv [(1 - w_2^{\mathrm{E}})\Delta\tilde{H}_{01} + w_2^{\mathrm{E}}\Delta\tilde{H}_{02} + \Delta_\beta\tilde{H}_{\mathrm{mix}}^{\mathrm{E}} - \Delta_\alpha\tilde{H}_{\mathrm{mix}}^{\mathrm{E}}]_{T=T_{\mathrm{E}}} \quad (28a) $$

and after having been substituted into eq 25 we get

$$ \Delta\tilde{H}_{\mathrm{E}} = \frac{w_2'' - w_2^\circ}{w_2'' - w_2^{\mathrm{E}}}\left[(1 - w_2^{\mathrm{E}})\Delta\tilde{H}_{01} + w_2^{\mathrm{E}}\Delta\tilde{H}_{02} + \Delta_\beta\tilde{H}_{\mathrm{mix}}^{\mathrm{E}} - \Delta_\alpha\tilde{H}_{\mathrm{mix}}^{\mathrm{E}} - \frac{w_2'' - w_2^{\mathrm{E}}}{w_2''' - w_2'''}\,{}_\alpha\tilde{H}''' - \frac{w_2^{\mathrm{E}} - w_2'''}{w_2''' - w_2'''}\,{}_\alpha\tilde{H}'' + {}_\alpha\tilde{H}^{\mathrm{E}}\right]_{T=T_{\mathrm{E}}} \quad (29) $$

where $\Delta\tilde{H}_{0i}$ denote the specific enthalpies of fusion of the pure components i ($i = 1, 2$) at the prevailing eutectic temperature T_{E}:

$$ [\Delta\tilde{H}_{0i}]_{T=T_{\mathrm{E}}} = [{}_\beta\tilde{H}_{0i} - {}_\alpha\tilde{H}_{0i}]_{T=T_{\mathrm{E}}} \quad (30) $$

These enthalpies must not be mistaken for the "real" (i.e. experimentally measurable) enthalpies of fusion $[\Delta\tilde{H}_{0i}]_{T_{\mathrm{m},i}}$ at the melting point $T_{\mathrm{m},i}$ inasmuch as those are hypothetical quantities obtained by extrapolating them from the melting point $T_{\mathrm{m},i}$ to lower temperatures (such as the eutectic temperature T_{E}) by means of the following general expression:[15]

$$ [\Delta\tilde{H}_{0i}]_{T_{\mathrm{E}}} = [\Delta\tilde{H}_{0i}]_{T_{\mathrm{m},i}} + [\Delta\tilde{c}_{p_{0i}}]_{T_{\mathrm{m},i}}(T_{\mathrm{E}} - T_{\mathrm{m},i}) + \int_{T_{\mathrm{E}}}^{T_{\mathrm{m},i}} \sum_{n=1}^{\infty} a_n (T - T_{\mathrm{m},i})^n \,\mathrm{d}T \quad (31) $$

Accordingly, a_n ($n = 1, 2, \ldots$) are empirical coefficients, and $[\Delta\tilde{c}_{p_{0i}}]_{T_{\mathrm{m},i}} = [{}_\beta\tilde{c}_{p_{0i}} - {}_\alpha\tilde{c}_{p_{0i}}]_{T_{\mathrm{m},i}}$ the differences of the specific heat capacities between state β (melt) and state α (crystal) of the pure components i ($i = 1, 2$) at $T = T_{\mathrm{m},i}$ and at constant pressure in which the specific heat capacities, $\tilde{c}_P$, are given by the definition

$$ \tilde{c}_P = (\partial\tilde{H}/\partial T)_P \quad (32) $$

Since the data of a_n are quite sparse, we disregard the temperature dependence of the specific heat capacities in eq 31 by setting $a_n = 0$, corresponding to a linear change of the enthalpies of fusion throughout the temperature interval involved. Furthermore, we conveniently ignore the temperature dependence of the enthalpies of fusion:

$$ \Delta\tilde{H}_{0i} \equiv [\Delta\tilde{H}_{0i}]_{T_{\mathrm{E}}} \approx [\Delta\tilde{H}_{0i}]_{T_{\mathrm{m},i}} \quad (33) $$

Equation 33 is not an unsatisfactory approximation at all, inasmuch as the heat capacities achieved by DSC measurements are sometimes more or less faithful. Hence, the error caused by leaving this temperature dependence out (being insignificant in any case) is mostly less serious than the attempt of considering this aforementioned dependence at all costs.

Finally, replacement of ${}_\alpha\tilde{H}'''$, ${}_\alpha\tilde{H}''$, and ${}_\alpha\tilde{H}^{\mathrm{E}}$ by the expressions derived according to eq 27 yields

$$ \Delta\tilde{H}_{\mathrm{E}} = \frac{w_2'' - w_2^\circ}{w_2'' - w_2^{\mathrm{E}}}[(1 - w_2^{\mathrm{E}})\Delta\tilde{H}_{01} + w_2^{\mathrm{E}}\Delta\tilde{H}_{02} + \Delta\Delta_{\alpha/\beta}\tilde{H}_{\mathrm{mix}}]_{T=T_{\mathrm{E}}} \quad (34a) $$

where

$$ \Delta\Delta_{\alpha/\beta}\tilde{H}_{\mathrm{mix}} = \Delta_\beta\tilde{H}_{\mathrm{mix}}^{\mathrm{E}} - \frac{w_2'' - w_2^{\mathrm{E}}}{w_2'' - w_2'''}\Delta_\alpha\tilde{H}_{\mathrm{mix}}''' - \frac{w_2^{\mathrm{E}} - w_2'''}{w_2'' - w_2'''}\Delta_\alpha\tilde{H}_{\mathrm{mix}}'' \quad (35a) $$

The reader can easily go through the few steps necessary to obtain eqs 34a and 35a. Note that the hypothetical enthalpy of maxing, $\Delta\tilde{H}_{\alpha\mathrm{mix}}^{\mathrm{E}}$, vanishes, since

$$ \left[-\frac{w_2'' - w_2^{\mathrm{E}}}{w_2'' - w_2'''}\,{}_\alpha\tilde{H}''' - \frac{w_2^{\mathrm{E}} - w_2'''}{w_2'' - w_2'''}\,{}_\alpha\tilde{H}'' + {}_\alpha\tilde{H}^{\mathrm{E}}\right]_{T=T_{\mathrm{E}}} \equiv \left[-\frac{w_2'' - w_2^{\mathrm{E}}}{w_2'' - w_2'''}\Delta_\alpha\tilde{H}_{\mathrm{mix}}''' - \frac{w_2^{\mathrm{E}} - w_2'''}{w_2'' - w_2'''}\Delta_\alpha\tilde{H}_{\mathrm{mix}}'' + \Delta_\alpha\tilde{H}_{\mathrm{mix}}^{\mathrm{E}}\right]_{T=T_{\mathrm{E}}} \quad (28b) $$

Equation 34a associated with eq 35a is the final expression of the specific eutectic enthalpy of fusion, $\Delta\tilde{H}_{\mathrm{E}}$, for an overall concentration $w_2^{\mathrm{E}} < w_2^\circ < w_2''$; however, it may also be applied to the other concentration range, $w_2''' < w_2^\circ < w_2^{\mathrm{E}}$, concerning the eutectic transition from state α to state γ if the phase indices or superscripts $('')$ and $(''')$ are swapped and state index or subscript β is formally replaced by γ:

$$ \Delta\tilde{H}_{\mathrm{E}} = \frac{w_2^\circ - w_2'''}{w_2^{\mathrm{E}} - w_2'''}[(1 - w_2^{\mathrm{E}})\Delta\tilde{H}_{01} + w_2^{\mathrm{E}}\Delta\tilde{H}_{02} + \Delta\Delta_{\alpha/\gamma}\tilde{H}_{\mathrm{mix}}]_{T=T_{\mathrm{E}}} \quad (34b) $$

with

$$ \Delta\Delta_{\alpha/\gamma}\tilde{H}_{\mathrm{mix}} = \Delta_\gamma\tilde{H}_{\mathrm{mix}}^{\mathrm{E}} - \frac{w_2'' - w_2^{\mathrm{E}}}{w_2'' - w_2'''}\Delta_\alpha\tilde{H}_{\mathrm{mix}}''' - \frac{w_2^{\mathrm{E}} - w_2'''}{w_2'' - w_2'''}\Delta_\alpha\tilde{H}_{\mathrm{mix}}'' \quad (35b) $$

2.2. Tammann's Triangle. The last section was devoted to quantitatively treating the eutectic transition. In this section we shall give a geometrical representation of all enthalpies involved herein, which is sketched in Figure 2 for the binary state diagram of Figure 1 as a function of the mass fraction of component 2. Points **A**, **E**, and **B** in Figure 2 therefore correspond to the labeled points in Figure 1. Furthermore, we shall look at eqs 34a and 34b in more detail. As we shall see, these relations may be viewed as a quantitative description of the so-called "Tammann's triangle".[13,16] In the next section we shall conclude the invariant eutectic transition with a brief digression to peritectic transitions, which may be treated by analogy.

Let us consider Figure 2. At $w_2 = 0$ and $w_2 = 1$, points P_1 and P_5 exhibit the ordinate values of the pure solid components

1 and 2, ${}_\alpha\tilde{H}''_{01} = {}_\beta\tilde{H}''_{01} = {}_\alpha\tilde{H}'''_{01} = {}_\beta\tilde{H}'''_{01}$ and ${}_\alpha\tilde{H}''_{02} = {}_\beta\tilde{H}''_{02} = {}_\alpha\tilde{H}'''_{02} = {}_\beta\tilde{H}'''_{02}$. These quantities are identical inasmuch as all of them are related to the solid state of the pure compounds indicated by superscript (″) or (‴). That is, despite different equilibrium states α, β, and γ underlying, a differentiation between these enthalpies thus becomes superfluous. Similarly, points P_6 and P_8 represent the enthalpies of the pure liquid components such that ${}_\beta\tilde{H}^{\mathrm{E}}_{01} = {}_\gamma\tilde{H}^{\mathrm{E}}_{01}$ and ${}_\beta\tilde{H}^{\mathrm{E}}_{02} = {}_\gamma\tilde{H}^{\mathrm{E}}_{02}$. The straight lines $\overline{P_1P_5}$ and $\overline{P_6P_8}$ correspond to additivity of the specific enthalpies of the pure solid components in state α and the liquid components in state β or γ. As, consequently, the distance between the points P_6 and P_1 characterizes the specific enthalpy of fusion of the pure component 1, $[\Delta\tilde{H}_{01}]_{T_{\mathrm{E}}}$, and that between points P_8 and P_5 is the specific enthalpy of fusion of the pure component 2, $[\Delta\tilde{H}_{02}]_{T_{\mathrm{E}}}$, the bracketed term in eq 34a or eq 34b minus $\Delta\Delta\tilde{H}_{\mathrm{mix}}$ (i.e. $\sum w_i^{\mathrm{E}}\Delta\tilde{H}_{0i}$) is determined by the distance between point P_7 and point P_3.

Curve a (P_1-**A**-**D**-**B**-P_5) describes the real behavior of the solid state α of an endothermic system favoring demixing in the solid state. At points **A**, **D**, and **B**, tangents to this curve afford the partial specific enthalpies of components 1 and 2 for the respective compositions of state α; that is, for w_2''', ${}_\alpha\tilde{H}'''_1$ and ${}_\alpha\tilde{H}'''_2$, for w_2^{E}, ${}_\alpha\tilde{H}^{\mathrm{E}}_1$ and ${}_\alpha\tilde{H}^{\mathrm{E}}_2$, and for w_2'', ${}_\alpha\tilde{H}''_1$ and ${}_\alpha\tilde{H}''_2$. Curve b (P_6-**E**-P_8) reflects the real situation of the liquid phase depicting a slightly exothermic behavior in our case which prefers a mixing of the liquid components. The tangent line constructed to curve b at point **E** thus yields the corresponding partial specific enthalpies of the two liquid components at the eutectic composition w_2^{E}: ${}_\beta\tilde{H}^{\mathrm{E}}_1 = {}_\gamma\tilde{H}^{\mathrm{E}}_1$ and ${}_\beta\tilde{H}^{\mathrm{E}}_2 = {}_\gamma\tilde{H}^{\mathrm{E}}_2$. Notice, only two points pertaining to curve a (points **A**, **B**) and a single point of curve β (point **E**) belong to stable coexisting phases.

We shall now consider eqs 4a, 4b, and 18, which have a simple geometrical interpretation in Figure 2. Equation 18 and the two identities of eq 4b characterize the quantities ${}_\alpha\tilde{H}^{\mathrm{E}}$ as well as ${}_\alpha\tilde{H}'''$ and ${}_\alpha\tilde{H}''$, corresponding to the ordinate values of point **D**, or points **A** and **B**, respectively. These quantities are the overall specific enthalpies of the individual phases at the relevant points; however, ${}_\alpha\tilde{H}^{\mathrm{E}}$ at point **D** belongs to a hypothetical *solid* phase with eutectic composition w_2^{E}. Equation 4a introduces the overall specific enthalpies of state β, namely, ${}_\beta\tilde{H}'$ (equivalent to ${}_\beta\tilde{H}^{\mathrm{E}}$) corresponding to the ordinate value of point **E**, and ${}_\beta\tilde{H}''$ that—despite being related to state β—represents the total specific enthalpy of the mixed crystal ***(II)*** and must therefore be equal to ${}_\alpha\tilde{H}''$ at point **B** (${}_\beta\tilde{H}'' = {}_\alpha\tilde{H}''$); in analogy to that, ${}_\gamma\tilde{H}''' = {}_\alpha\tilde{H}'''$ must hold at point **A**. With these enthalpies at hand, we are also capable of determining the above "enthalpies of transfer" from Figure 2: $\Delta\tilde{H}_{\mathrm{III}\to\mathrm{E}} \equiv ({}_\alpha\tilde{H}''' - {}_\alpha\tilde{H}^{\mathrm{E}})$ is the difference between point **A** and point **D** (here negative); $\Delta\tilde{H}_{\mathrm{II}\to\mathrm{E}} \equiv ({}_\alpha\tilde{H}'' - {}_\alpha\tilde{H}^{\mathrm{E}})$ corresponds to the difference between **B** and **D** (here positive). Considering eq 26, we may also assign the distances $\overline{\mathbf{A}-P_2}$, $\overline{\mathbf{C}-P_3}$, and $\overline{\mathbf{B}-P_4}$ to the specific enthalpies of mixing, $\Delta_\alpha\tilde{H}'''_{\mathrm{mix}}$, $\Delta_\alpha\tilde{H}^{\mathrm{E}}_{\mathrm{mix}}$, and $\Delta_\alpha\tilde{H}''_{\mathrm{mix}}$, and distance $\overline{\mathbf{E}-P_7}$ to $\Delta_\beta\tilde{H}^{\mathrm{E}}_{\mathrm{mix}}$, which is equivalent to $\Delta\tilde{H}^{\mathrm{E}}_{\gamma\mathrm{mix}}$.

It is evident from eq 2b combined with eq 3b, or eq 2a combined eq 3a, that the sum of ${}_\alpha\tilde{H}'''$ (point **A**) and ${}_\alpha\tilde{H}''$ (point **B**), or ${}_\beta\tilde{H}^{\mathrm{E}}$ (point **E**) and ${}_\beta\tilde{H}''$ (point **B**), weighed by the phase mass ratio, ${}_\epsilon m^\delta/m$, of the relevant phase $\delta = ({}^{\mathrm{E}})$, (″), (‴) in the state $\epsilon = \alpha$, β yields the total specific enthalpies of state α or state β, ${}_\alpha\tilde{H}_{T_{\mathrm{E}}}$ or ${}_\beta\tilde{H}_{T_{\mathrm{E}}}$, respectively. Analogously, the overall specific enthalpy of the other solid−liquid equilibrium γ ($\epsilon = \gamma$) prevailing beyond the eutectic point in Figure 1, ${}_\gamma\tilde{H}_{T_{\mathrm{E}}}$, results from ${}_\gamma\tilde{H}'''$ (point **A**) and ${}_\gamma\tilde{H}^{\mathrm{E}}$ (point **E**). Hence, line $\overline{\mathbf{E}-\mathbf{B}}$ and line $\overline{\mathbf{A}-\mathbf{E}}$ in Figure 2 characterize all solid−liquid equilibria β and γ for $w_2^{\mathrm{E}} < w_2^\circ < w_2''$, or $w_2''' < w_2^\circ < w_2^{\mathrm{E}}$, respectively, and line $\overline{\mathbf{A}-\mathbf{B}}$ characterizes the solid−solid equilibrium α of the two coexisting mixed crystals ***(III)*** and ***(II)***, as depicted in Figure 2. At a given overall composition w_2° the total enthalpy change during the eutectic transition, $\Delta\tilde{H}_{\mathrm{E}}$, which is defined either by eq 1a for $w_2^{\mathrm{E}} < w_2^\circ < w_2''$ (transition $\alpha \to \beta$) or by eq 1b for $w_2''' < w_2^\circ < w_2^{\mathrm{E}}$ (transition $\alpha \to \gamma$), is thus given by the distance between the lines $\overline{\mathbf{E}-\mathbf{B}}$ and $\overline{\mathbf{C}-\mathbf{B}}$, such as distance $\overline{P_{10}P_9}$ in Figure 2, or between $\overline{\mathbf{A}-\mathbf{E}}$ and $\overline{\mathbf{A}-\mathbf{C}}$. It is largest at the eutectic composition $w_2^\circ = w_2^{\mathrm{E}}$, corresponding to the distance $\overline{\mathbf{E}-\mathbf{C}}$ in Figure 2 or to the bracketed term in eq 34a. For this reason, as distance $\overline{\mathbf{E}-P_7}$ signifies $\Delta_\beta\tilde{H}^{\mathrm{E}}_{\mathrm{mix}}$ or $\Delta_\gamma\tilde{H}^{\mathrm{E}}_{\mathrm{mix}}$, as has been shown above, the difference of the ordinate values between points **C** and P_3 must comply with the last two terms in eqs 35a or 35b. For the purpose of illustration, however, the enthalpies of mixing have been drawn in Figure 2 quite markedly. In reality, the courses of curves a and b are much flatter owing to $\Delta\tilde{H}_{0i} \gg \Delta_\epsilon\tilde{H}^\delta_{\mathrm{mix}}$ ($i = 1, 2$; $\delta = {}^{\mathrm{E}}, '', '''$; $\epsilon = \alpha, \beta, \gamma$) so that $\Delta\Delta_{\alpha/\beta}\tilde{H}_{\mathrm{mix}}$ and $\Delta\Delta_{\alpha/\gamma}\tilde{H}_{\mathrm{mix}}$ may usually be neglected. Moreover, in case of points **A** and **B** shifted toward the ordinates (i.e. $w_2''' \to 0$ and $w_2'' \to 1$ in Figure 1 or Figure 2) corresponding to a decrease in solid solubility, $\Delta_\alpha\tilde{H}'''_{\mathrm{mix}}$ and $\Delta_\alpha\tilde{H}''_{\mathrm{mix}}$ vanish anyway (due to the shift of **A** to P_1 and of **B** to P_5 in Figure 2).

We hence reach the following conclusions from eqs 34a−35b and Figure 2: The bracketed terms in eqs 34a and 34b correspond to the maximum specific eutectic enthalpy of fusion at the eutectic point. With growing distance from this point, i.e. the more the initial composition w_2° differs from the eutectic composition w_2^{E}, the more the eutectic enthalpy decreases until it vanishes at composition w_2''' or w_2''. However, it must be observed that only the phase mass ratio is subject to change hereby and *never* the compositions of the three coexisting phases (w_2''', w_2^{E}, and w_2''). These phase mass ratios ${}_\beta m^{\mathrm{E}}/m$ or ${}_\gamma m^{\mathrm{E}}/m$, by which the bracketed terms in eqs 34a and 34b are diminished, are identical with the respective front factors, $(w_2'' - w_2^\circ)/(w_2'' - w_2^{\mathrm{E}}) \le 1$ or $(w_2^\circ - w_2''')/(w_2^{\mathrm{E}} - w_2''') \le 1$; the numerator is equivalent to the mass of the eutectic melt, and the denominator corresponds to the total mass of the sample used.

Consequently, $\Delta\tilde{H}_{\mathrm{E}}$ is observed to depend linearly on the initial composition w_2°, since w_2''', w_2^{E}, and w_2'' are constant quantities. By plotting $\Delta\tilde{H}_{\mathrm{E}}$ versus w_2°, two straight lines result, intersecting each other at the eutectic point **E** (w_2^{E}), where the eutectic enthalpy becomes maximum, and intersecting with the abcissa at points **A** (w_2''') and **B** (w_2''), where the eutectic enthalpy vanishes. Equations 34a and 34b may therefore be considered as a quantitative description of Tammann's procedure following general principles.[13,16] They furnish a triangle, similar to that shown in Figure 2 (**A**−**E**−**B**), and facilitate deciding from experimental data whether a miscibility gap of the solid components within the state α is extended to the ordinates characterized by $w_2 = 0$ and $w_2 = 1$ or whether a more or less distinct solubility does exist upon forming mixed crystals. A relationship equivalent to eqs 34a and 34b, but obtained by a somewhat different formalism, has been derived by Borchard et al., who besides considered an additional phase comprising a certain amount of the nontransformed, initially homogeneous phase due to kinetical hindrance on cooling.[17]

As can be seen from eqs 34a and 35a, the eutectic composition w_2^{E} is, in principle, predictable if the respective quantities, such as the specific enthalpies of fusion of the pure components and the specific eutectic enthalpy as a function of the prevailing initial composition w_2°, are known. Using, for instance, eqs 34a and 35a, we get

$$w_2^{\mathrm{E}} = [w_2''\Gamma - (w_2'' - w_2''')(\Delta\tilde{H}_{01} + \Delta_\beta\tilde{H}_{\mathrm{mix}}^{\mathrm{E}}) + w_2''\Delta_\alpha\tilde{H}_{\mathrm{mix}}''' - w_2'''\Delta_\alpha\tilde{H}_{\mathrm{mix}}''']/[\Gamma + (w_2'' - w_2''')(\Delta\tilde{H}_{02} - \Delta\tilde{H}_{01}) + \Delta_\alpha\tilde{H}_{\mathrm{mix}}''' - \Delta_\alpha\tilde{H}_{\mathrm{mix}}''] \quad (36a)$$

where

$$\Gamma \equiv \frac{w_2'' - w_2'''}{w_2'' - w_2^\circ}\Delta\tilde{H}_{\mathrm{E}} = \mathrm{const} \quad (36b)$$

However, it should be emphasized that the determination of the eutectic composition by means of eq 36a is fairly delicate with respect to inaccuracies in the eutectic enthalpy of fusion. Strictly speaking, the more w_2° differs from w_2^{E} the larger the standard deviation in w_2^{E} calculated by means of eq 36a because the eutectic peak continually disappears in the noise of the DSC curve. As, in addition, its width is markedly affected by the initial composition,[4] yielding less faithful values in $\Delta\tilde{H}_{\mathrm{E}}$ with growing distance between w_2° and w_2^{E}, the eutectic composition (but also $w_2'''$and w_2'') should always be established from many experimental data, being as large in number as possible (linear regression).

2.3. Peritectic Transitions of Fusion. So far we have only dealt with the eutectic transition. To complete the picture, we wish to demonstrate that the invariant peritectic transition may be treated with the same formalism. Similarly to that, a peritectic equilibrium is characterized by the coexistence of three phases at the peritectic temperature T_{P}, namely, the liquid (peritectic) phase at the peritectic point **P** (with the peritectic composition w_2^{P}) and the two solid phases at points **A** and **B** with the compositions w_2''' and w_2', respectively. However, instead of being located *between* the compositions of the two solid phases, i.e. *within* the miscibility gap $\overline{\mathbf{A}-\mathbf{B}}$ of the solid state as sketched in Figure 1 for the eutectic transition, the peritectic melt is located *beyond* the two solid phases, i.e. *outside* this miscibility gap, so that $0 < w_2^{\mathrm{P}} < w_2''' < w_2'' < 1$. Since we shall not dwell more on peritectic phase diagrams, we abstain from an illustration; for a more comprehensive picture, the reader is referred to textbooks of thermodynamics. Hence, there are two states to be distinguished beneath T_{P}: a solid−liquid equilibrium γ and a solid−solid equilibrium α. Above T_{P}, only one single state exists: a solid−liquid equilibrium β. In the case of the transition $\alpha \rightarrow \beta$ (for $w_2''' < w_2^\circ < w_2''$) the final expression for the specific peritectic enthalpy of fusion, $\Delta\tilde{H}_{\mathrm{P}}$, may be obtained from eqs 34a and 35a if index ($^{\mathrm{P}}$) is substituted for index ($^{\mathrm{E}}$). In the case of the other transition $\gamma \rightarrow \beta$ where $w_2^{\mathrm{P}} < w_2^\circ < w_2'''$, the relevant relationship for $\Delta\tilde{H}_{\mathrm{P}}$ may be shown to be equivalent to eqs 34b and 35b by replacing superscript (‴) by ($^{\mathrm{P}}$), superscript ($^{\mathrm{E}}$) by (″), and superscript (″) by (‴). In analogy to the eutectic transition, Tammann's triangle will also be achieved, which becomes maximum, however, at point **A** (i.e. if w_2° equals the composition w_2''' of the mixed crystal ***(III)***) and *not* at the peritectic compsition w_2^{P}.

2.4. Transition of Fusion of the Remaining Crystal (λ-Transition). The last three sections have dealt with invariant transitions at one single temperature, such as the eutectic transition of fusion at the eutectic temperature T_{E}. In this section we look at the transition of fusion (λ-transition) of the remaining crystal ***(II)*** or ***(III)***, respectively, which may, on one hand, succeed a eutectic transition if the pure compounds are not completely miscible throughout the entire concentration range. If, on the other hand, a complete series of solid solution is prevailing, the eutectic transition is absent and only a melting transition of a mixed crystal occurs. Note, this transition is no longer fixed at one temperature, and it reveals a more or less broad range of fusion running from the eutectic temperature to the melting point of the binary mixture at temperature T_{m}. For this reason, the temperature dependence of the relevant enthalpies and compositions must, in addition, be taken into account. Supposing the former case with a eutectic transition were applicable, as sketched in Figure 1, we would have to distinguish between a transition with respect to state β or γ. Thus, only the superscripts (′) and (″) are conveniently employed for the melt ***(I)*** and for the mixed crystal, but bearing in mind that (″) needs to be replaced by (‴) if equilibrium γ between the melt and the mixed crystal ***(III)*** is considered. In this respect it is irrelevant to the following derivation whether complete solubility, partial solubility, or even no solubility within the solid state is actually underlying.

Similarly to the foregoing section, we set about considering the total extensive enthalpy, $H(T)$, of the two-phase system at temperature T ranging from T_{E} (onset) to the end of melting of the respective crystal at temperature T_{m}. Starting out from eq 2a and omitting state index β in all following equations, we get

$$H(T) = H'(T) + H''(T) \quad (2c)$$

with the extensive enthalpies of the melt (′), $H'(T)$, and of the solid phase (″), $H''(T)$. Recalling eqs 3a and 4a, we find in analogy to eq 5a

$$H(T) = m'[w_1'\tilde{H}_1' + w_2'\tilde{H}_2'] + m''[w_1''\mathrm{H}_1'' + w_2''H_2'' \quad (5c)$$

where $\tilde{H}_i' = \tilde{H}_i'(w_i',T)$ and $\tilde{H}_i'' = \tilde{H}_i''(w_i'',T)$ denote the partial specific enthalpies, $w_i' = w_i'(T)$ and $w_i'' = w_i''(T)$, the mass fractions of component i (with $i = 1, 2$) with respect to phase (′) or (″) and the temperature T. In case no solubility within the solid state is observed, which in turn leads to a melting transition of a crystal consisting of either the pure component 1 or the pure component 2, eq 32 will be reduced by taking $w_2'' = 0$ and $\tilde{H}_1'' = \tilde{H}_{01}''$ or $w_2'' = 1$ and $\tilde{H}_2'' = \tilde{H}_{02}''$, respectively.

Application of the lever rule owing to eqs 9a and 10a with superscript ($^{\mathrm{E}}$) replaced by (′) and introduction of the enthalpies of mixing pursuant to eq 27 give the overall specific enthalpy, $\tilde{H}(T)$, of the state at any temperature T:

$$\tilde{H}(T) = \frac{w_2'' - w_2^\circ}{w_2'' - w_2'}[(1 - w_2')\tilde{H}_{01}' + w_2'\tilde{H}_{02}' + \Delta\tilde{H}_{\mathrm{mix}}'] + \frac{w_2^\circ - w_2'}{w_2'' - w_2'}[(1 - w_2'')\tilde{H}_{01}'' + w_2''\tilde{H}_{02}'' + \Delta\tilde{H}_{\mathrm{mix}}''] \quad (37)$$

In view of the fact that enthalpies are dependent on temperature, we apply the definition of specific heat capacity (eq 32) to eq 37, where all quantities, apart from the initial composition w_2°, require to be taken as a function of temperature. Hence, the final expression of the specific heat reads for the regarded state of the two-phase system

$$\tilde{c}_P(T) = \tilde{c}_P^{\mathrm{base}}(T) + \tilde{c}_P^{\mathrm{melt}}(T) \quad (38a)$$

where

$$\tilde{c}_P^{\mathrm{base}}(T) = \frac{w_2'' - w_2^\circ}{w_2'' - w_2'}\left[(1 - w_2')\tilde{c}_{P_{01}}' + w_2'\tilde{c}_{P_{02}}' + \left(\frac{\partial\Delta\tilde{H}_{\mathrm{mix}}'}{\partial T}\right)_P\right] + \frac{w_2^\circ - w_2'}{w_2'' - w_2'}[(1 - w_2'')\tilde{c}_{P_{01}}'' + w_2''\mathrm{c}_{P_{02}}'' + \left(\frac{\partial\Delta\tilde{H}_{\mathrm{mix}}''}{\partial T}\right)_P \quad (38b)$$

and

$$\tilde{c}_P^{\mathrm{melt}}(T) = \frac{w_2'' - w_2^\circ}{(w_2'' - w_2')^2}\left(\frac{\partial w_2'}{\partial T}\right)_P[(1 - w_2'')\Delta\tilde{H}_{01} + w_2''\Delta\tilde{H}_{02} + \Delta\tilde{H}'_{\mathrm{mix}} - \Delta\tilde{H}''_{\mathrm{mix}}] + \frac{w_2^\circ - w_2'}{(w_2'' - w_2')^2}\left(\frac{\partial w_2''}{\partial T}\right)_P[(1 - w_2')\Delta\tilde{H}_{01} + w_2'\Delta\tilde{H}_{02} + \Delta\tilde{H}'_{\mathrm{mix}} - \Delta\tilde{H}''_{\mathrm{mix}}] \quad (38c)$$

All quantities are hereby related to the prevailing temperature T except for w_2°: $\tilde{c}_{P01}^{\delta}$ and $\tilde{c}_{P02}^{\delta}$ denote the specific heat capacities of the pure components 1 and 2 with reference to the liquid state ($\delta = '$) or the crystalline state ($\delta = ''$), $\Delta\tilde{H}_{01}$ and $\Delta\tilde{H}_{02}$ are the enthalpies of fusion that may roughly be determined by eq 31 substituting $T_{\mathrm{m},i}$ for T_{E}, $\Delta\tilde{H}'_{\mathrm{mix}}$ and $\Delta\tilde{H}''_{\mathrm{mix}}$ designate the enthalpies of mixing of the liquid or the solid mixture with respect to the prevailing composition w_2' or w_2'', respectively, and $(\partial w_2'/\partial T)_P$ or $(\partial w_2''/\partial T)_P$ are the reciprocal slopes of the liquidus or the solidus curve of the underlying phase diagram depicting temperature versus composition (see Figure 1). For the sake of clarity, however, we dropped a particular indication of temperature of these quantities in eqs 38b and 38c.

Equation 38a comprises two contributions to the overall specific heat capacity at temperature T: $\tilde{c}_P^{\mathrm{base}}(T)$ and $\tilde{c}_P^{\mathrm{melt}}(T)$. The former, termed "base line", gives the thermodynamic expression of the temperature-dependent change of enthalpy of both the melt and the coexisting crystal whose (actual) compositions, $w_2'(T)$ and $w_2''(T)$, are represented by the liquidus and solidus curves. Drawing a comparison to previous methods described in the literature,[18−22] eq 38b should thus be more suitable to construct the precise base line of every binary DSC curve based on the condition, however, that the thermodynamic quantities necessary are known. The construction of approximate base lines to almost any DSC diagram—inclusive of "smeared" DSC curves—will be taken up again in part 4 of this series, where the knowledge of the inidividual thermodynamic quantities will not be required.[6] On the other hand, $\tilde{c}_P^{\mathrm{melt}}(T)$ signifies the enthalpy change of the melt and the crystal at temperature T owing to fusion. We may therefore attribute the first terms in eqs 38b and 38c to the influence of the liquidus curve, and their second terms to the influence of the solidus curve.

In conclusion, we would like to point out that this set of equations (eqs 38a−38c), despite being derived for a melting transition of a binary crystal as an example, are universally applicable to any phase transition of a binary mixture (such as evaporation and sublimation, but also mixing−demixing phenomena[23]) showing a λ-point[1−3,24] in phenomenological terms. In these cases, "$\tilde{c}_P^{\mathrm{melt}}(T)$" always corresponds to the change of enthalpy of the proper transition ("melt" should be replaced then by the relevant indices "vap", etc.); for instance, if mixing or demixing is considered, $\Delta\tilde{H}_{0i} = 0$ so that "$\tilde{c}_P^{\mathrm{melt}}(T)$" is exclusively dependent on intermolecular interaction forces represented in eq 38c by the specific enthalpies of mixing of the two coexisting phases. Contrary to previous approaches to a calculation of DSC curves given in the literature,[25,26] the above relationships of this section look at the change of enthalpy due to a rise in temperature, aside from considering the change of enthalpy due to a change of the phase mass ratios according to the lever rule.

2.5. Thermal Behavior of the Melt. The homogeneous region of the melt ***(I)*** will be reached if the very last residue of the remaining crystal ***(II)*** or ***(III)*** has entirely been molten. Because only the liquid phase ($'$) is present, the overall specific enthalpy at the temperature $T_{\mathrm{m}} < T < T_{\mathrm{II}}$ (see Figure 1) is thus found to be

$$\tilde{H}'(T) = (1 - w_2^\circ)\tilde{H}_1' + w_2^\circ\tilde{H}_2' \quad (39)$$

or if eq 27 has been taken with the superscript ($^{\mathrm{E}}$) replaced by ($'$),

$$\tilde{H}'(T) = (1 - w_2^\circ)\tilde{H}_{01}' + w_2^\circ\tilde{H}_{02}' + \Delta\tilde{H}'_{\mathrm{mix}} \quad (40)$$

Using eq 32 affords the final expression

$$\tilde{c}_P'(T) = (1 - w_2^\circ)\tilde{c}'_{P_{01}} + w_2^\circ\tilde{c}'_{P_{02}} + \left(\frac{\partial\Delta\tilde{H}'_{\mathrm{mix}}}{\partial T}\right)_P \quad (41)$$

that may also be achieved from eqs 38a−38c by setting $w_2' = w_2^\circ$ = constant. Equation 41 describes the temperature-dependence of the specific heat of the homogeneous melt ($'$) at the respective temperature T.

2.6. Thermal Behavior of the Solid State. Let us end our thermodynamic considerations with a description of the thermal behavior of the solid state preceding the actual transition of fusion. Because this state may appear to be both, separated into two crystals coexisting with one another (two phases) or being a complete solid solution (one phase), several cases need to be distinguished quite accurately. In the latter case, we get from eqs 38a−38c by taking $w_2'' = w_2^\circ$ = constant

$$\tilde{c}_P''(T) = (1 - w_2^\circ)\tilde{c}''_{P_{01}} + w_2^\circ\tilde{c}''_{P_{02}} + \left(\frac{\partial\Delta\tilde{H}''_{\mathrm{mix}}}{\partial T}\right)_P \quad (42)$$

Equation 42 involves almost all cases of complete series of mixed crystals. It is equivalent to eq 41, differing only in their superscripts ($''$) and ($'$).

In contrast to that, the solid phase may display a demixing into two crystals. At low temperatures, two mixed crystals whose compositions are characterized by the solid−solid miscibiliy gap should be observed; the former consists of two branches (solvus curves) that terminate, for example, either in the upper critical point (UCP) or—in case a eutectic type of phase diagram with a partially demixed solid state exists—in the points **A** and **B** at the eutectic temperature T_{E}, as shown in Figure 1. In this latter case, **A** and **B** are the points of intersection of the solidus and solvus curves. Thus, the heterogeneous phase behavior of both the crystal ***(III)*** and the crystal ***(II)*** should actually be described by means of eqs 38 by replacing superscript ($'$) with ($'''$). Since, however, mixed crystals do not establish equilibrium compositions instantaneously by following the solvus curves—due to an extremely slow diffusion in crystals[9,27]—these solid−solid equilibria are not approached during of a DSC scan. Additionally, as the solvus curves are fairly steep generally—resulting in $(\partial w_2^\gamma/\partial T)_P \rightarrow 0$ ($\gamma = ', ''$) and $\tilde{c}_P^{\mathrm{melt}}(T) \rightarrow 0$ (see eqs 38)—the course of the DSC curve scanned in this range (i.e. the range from the onset of the scan to the onset of the melting transition) can approximately be described by eq 42, in which the mixing term has been ruled out.

3. Experimental Section

Hydrocarbons used were *n*-eicosane (n-C_6H_{14}) and *n*-triacontane (n-$C_{12}H_{26}$) from Aldrich-Chemie, Steinheim, without further purification. Each sample has been crystallized with a cooling rate of about 0.3 K·min^{-1}. Scans have been performed on a differential scanning calorimeter (DSC-2C) from Perkin-Elmer with a heating rate of 10 K·min^{-1}. The melting temperatures of the samples, T_{m}, were evaluated as those corresponding to the right foot point of the fusion peak.

4. Computation of the DSC Curves

The DSC traces of our model system chosen, consisting of *n*-hexane (n-C_6H_{14}) and *n*-dodecane (n-$C_{12}H_{26}$), have been

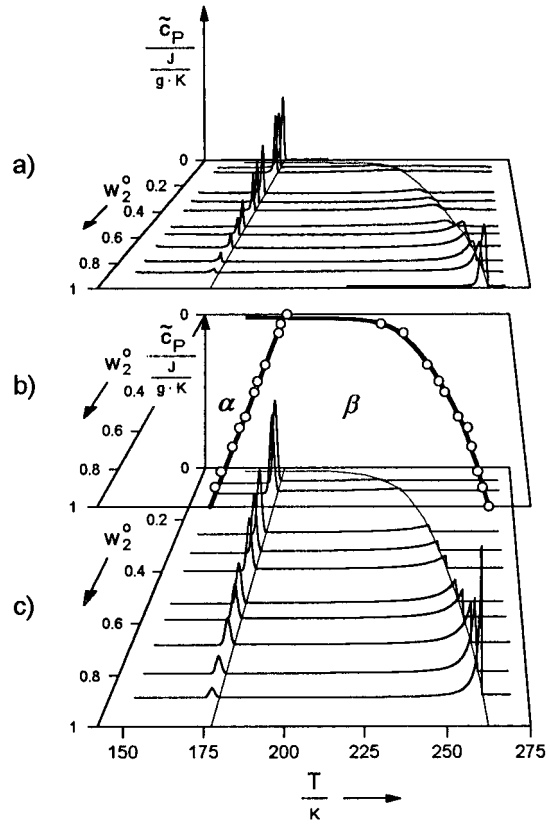

Figure 3. Binary system consisting of *n*-hexane (n-C_6H_{14}) and *n*-dodecane (n-$C_{12}H_{26}$): (a) experimental DSC scans (heating rate 10 $K \cdot min^{-1}$) depicting the specific heat capacity against temperature and graded by increasing overall compositions w_2° toward the front; (thin solid line) eutectic temperatures (T_E) and liquidus temperatures (T_m); (b) isobaric state diagram arising out of a projection of the eutectic and liquidus temperatures of Figure 3a to the $T-w_2^\circ$ plane; (c) calculated DSC curves according to the thermodynamic relations derived (see text).

computed using the following equations: First, we adopted eqs 38 to describe the temperature range prior to the eutectic transition. After substituting indices (‴) for (′) and due to constant compositions of the two solid phases ($w_2'''= 0$; $w_2''' = 1$), eqs 38 reduced to a relationship that is formally equivalent to eq 42 if the mixing term is dropped. The specific eutectic enthalpies of fusion have been calculated by means of eqs 34a and 35a with $w_2'''$and w_2'' taken to be 0 or 1, respectively, and with the eutectic composition w_2^E assumed to be 0.001 (see Figure 3b). As we have seen, the "ideal" (nonsmeared) traces of the eutectic fusion peaks should show an infinitely sharp transition with an apparently infinite value of the specific heat capacity. In order to render them representable but also to fit them to real (smeared) conditions, we used Gaussian distributions that have turned out to describe experimental eutectic peaks sufficiently. Here, their widths (ΔT) approximately correspond to the widths of the fusion peaks of the two pure components taken at the *foot* thereof, and T_E is the temperature where the eutectic transition is completed, so that the onset of the simulated eutectic peaks must always be located at the temperature ($T_E - \Delta T$). The eutectic peak heights have thus required to be taken as a function of the eutectic enthalpy of fusion; the relevant relationships between the peak area and the parameters of a Gaussian distribution will, however, be given in the third part of this series.[5] As we shall see, the peak width of a eutectic transition is, strictly speaking, also conditional on the initial composition.[4]

The transition peaks of the remaining crystal (λ-transition), succeeding the eutectic transition within the temperature range between T_E and T_m, have been calculated from eqs 38a−38c

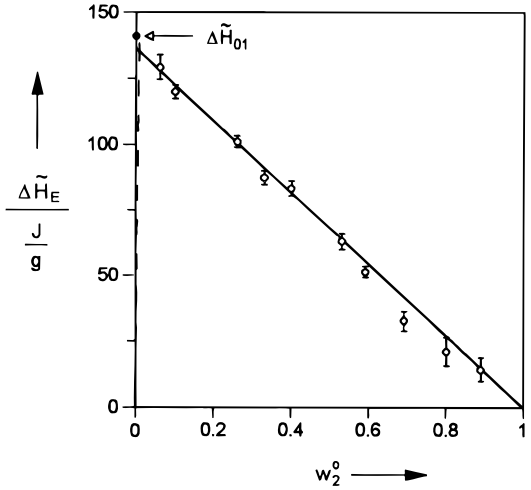

Figure 4. Dependence of the experimental specific eutectic enthalpy of fusion $\Delta\tilde{H}_E$ upon the initial composition w_2° (see text). The dashed straight line indicates the left-hand side of Tammann's triangle (hypothetical, not measured); the vertical bars signify the margin of error.

with the reduction $w_2'' = 1$ and the approximation of eq 33. The necessary values for temperature and composition of the liquid phase, T and w_2', have hereby been obtained by scanning the liquidus curve smoothed within the compositions ranging from w_2^E to w_2°. Although eq 38a represents the specific heat capacity at a distinct temperature T and composition w_2', we approximately assigned the reciprocal slope of the liquidus curve, $(\partial w_2'/\partial T)_P$, assumed to be about $(\Delta w_2'/\Delta T)_P$, to the interval between $(w_2' - \Delta w_2')$ and w_2', where $\Delta w_2'$ designates the width which has arbitrarily been set to 1×10^{-3} while $\Delta T = T(w_2') - T(w_2' - \Delta w_2')$. Hence, the change of the specific enthalpy in this interval could be considered as $\Delta\tilde{H} \approx \tilde{c}_p(w_2')\Delta T$. Finally, the specific heat capacity of the homogeneous melt (at $T > T_m$) was furnished from eq 41.

It must be emphasized that all underlying calculations have been carried out by disregarding the (unknown) enthalpies of mixing; this is allowed insofar as a nonpolar model system is present. Moreover, as it is exceedingly hard to achieve faithful experimental data of the specific heat capacities by DSC experiments, we roughly assigned the specific standard heat capacities, $\tilde{c}^\circ_{P_{01}}$ and $\tilde{c}^\circ_{P_{02}}$[28], referred to a unit pressure of 1 atm (1.013 bar) and a temperature of 298 K, to those quantities related to the liquid state,

$$\tilde{c}'_{P_{01}} \equiv \tilde{c}^\circ_{P_{01}} = 2.27\ J \cdot g^{-1} \cdot K^{-1} \tag{43a}$$

$$\tilde{c}'_{P_{02}} \equiv \tilde{c}^\circ_{P_{02}} = 2.21\ J \cdot g^{-1} \cdot K^{-1} \tag{43b}$$

whereas the quantities for the solid state have arbitrarily been equated to

$$\tilde{c}''_{P_{01}} \equiv 0.27\ J \cdot g^{-1} \cdot K^{-1} \tag{44a}$$

$$\tilde{c}''_{P_{02}} \equiv 0.21\ J \cdot g^{-1} \cdot K^{-1} \tag{44b}$$

corresponding to a discontinuity of $\Delta\tilde{c}_{P_{0i}} \approx 2\ J \cdot (g \cdot K)^{-1}$ at each melting point, evaluated from the experimental curves of the pure paraffins. These quantities have further been taken to remain constant throughout the entire temperature range since their temperature-dependence has also been unknown.

5. Results and Discussion

Figures 3 and 4 display our results concerning the binary system n-C_6H_{14}/n-$C_{12}H_{26}$ investigated. Figure 3a shows the

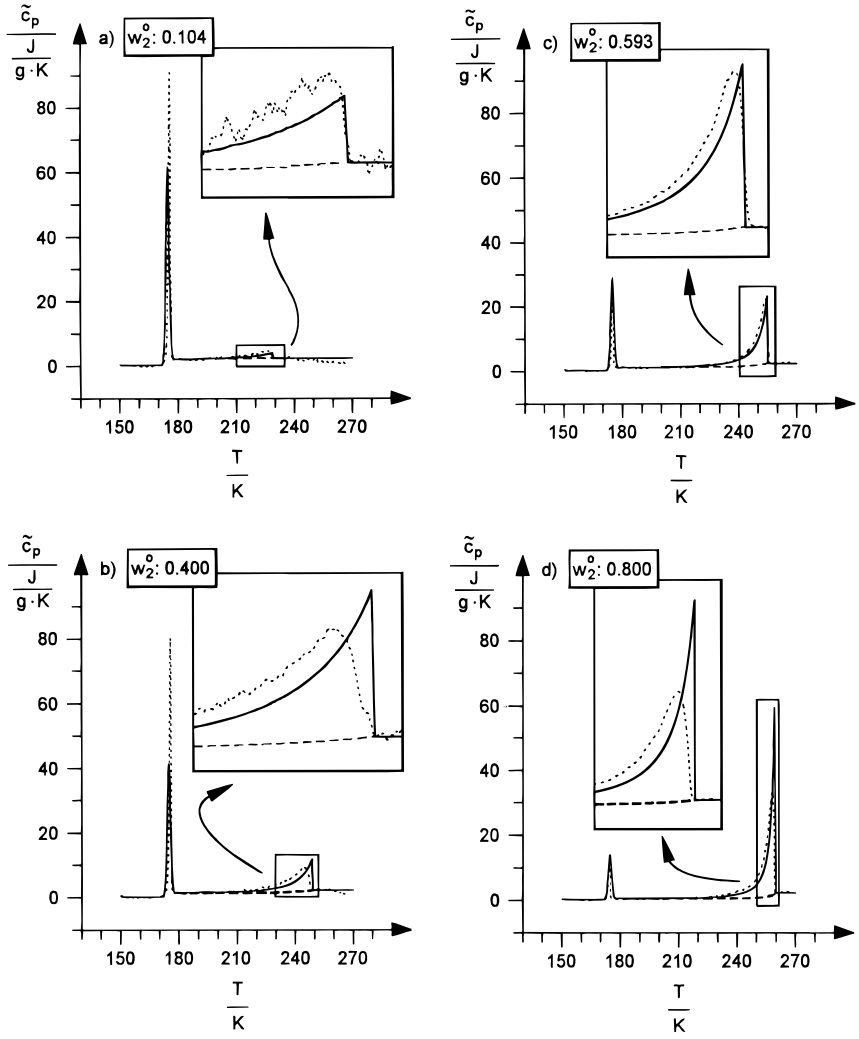

Figure 5. Diagram showing the calculated DSC curves (solid) with the respective base lines (dashed) and the experimental DSC curves (dotted) as a function of the initial concentration w_2^o: 0.104 (a), 0.400 (b), 0.593 (c), 0.800 (d).

experimental DSC curves of various binary mixtures obtained by heating with a scan speed of 10 K·min^{-1}. By plotting the temperatures of fusion evaluated as those corresponding to the peak ends against the overall mass fraction w_2^o of component 2 (n-$C_{12}H_{26}$), the resulting state diagram is achieved, as depicted in Figure 3b. Clearly, the eutectic concentration is shifted toward lower concentrations so that state β is approached only ($w_2^E \rightarrow 0$) and the eutectic point **E** is nearly identical with the melting point $T_{m,1}$ of the lower molecular component (n-C_6H_{14}). This complies with the results shown in Figure 4, where the influence of the initial concentration w_2^o on the eutectic enthalpy of fusion has been investigated. Linear extrapolation of these data leads to a single straight line that intersects with the abscissa at approximately $w_2^o = 1$ and the ordinate at a value that is almost equivalent to the enthalpy of fusion of component 1 (n-C_6H_{14}). Note, this Tammann's "triangle" obtained (Figure 4) results from Figure 2 if points **E** and P_6 (and also points **C** and P_1) coincide at $w_2''' = 0$, while, on the other hand, point **B** becomes identical with point P_5 at $w_2''' = 1$. In this respect, since $w_2''' = 0$, $w_2'' = 1$, and $w_2^E \rightarrow 0$ so that $\Delta\tilde{H}_E \approx \Delta\tilde{H}_{01}$, no solid solubility should exist in state β (see Figure 3b and section 2.1).

Starting out with the phase diagram drawn in Figure 3b and taking the above reductions into account, we were able to compute the desired DSC curves, depicted in Figure 3c. Besides that, four simulated DSC curves (solid lines) with initial compositions 0.104, 0.400, 0.593, and 0.800 are demonstrated in Figure 5, each of which contains an enlargement of the region around the end of the fusion peak. Obviously, the increase of the specific heat capacity immediately after the eutectic transition at T_E, compared with those being prior, is greater the closer the overall composition w_2^o is located to the eutectic composition inasmuch as the influence of the heat capacities $\tilde{c}'_{P_{01}}$ and $\tilde{c}'_{P_{02}}$ of the liquid phase is becoming more marked owing to an increasingly larger quantity of the melt.[6] This may also be shown for the experimental DSC curves already displayed in Figure 3a as well as in Figure 5 (dotted lines). In the interest of a better comparability, however, the original DSC curves have further been tilted before so that the magnitude of the specific heat capacities are nearly equivalent to those calculated at the onset of the eutectic transition and at the end of the subsequent transition. This might be allowed insofar as the heat capacities obtained by DSC are not very trustworthy anyway (due to the intermediate phases that do not attain equilibrium states immediately). At the same time the dashed lines in Figure 5 represent the theoretical (exact) base lines in terms of thermodynamics that have been calculated by eq 38b. Indeed, base lines serve to determine the peak area of any DSC curve by integration. As outlined above, they characterize both the quantity already fused and the crystalline quantity that does not undergo fusion at the prevailing temperature T ($T_E < T < T_m$).

Comparison with the experimental data reveals that the computed DSC curves are in a good agreement with those obtained by experiments, at least in a semiquantitative way. However, the widths of the eutectic peaks and hence the peak

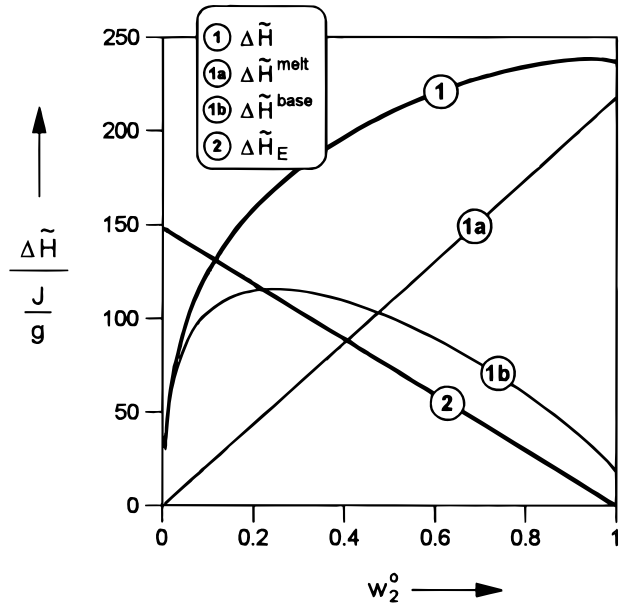

Figure 6. Diagram depicting the course of various contributions to the enthalpy of fusion plotted against the overall composition w_2° (see text). Curve 1: total specific enthalpy of fusion being the sum of the specific enthalpy of fusion of the binary mixture (curve 1a) and the contribution of the base line (curve 1b). Curve 2: specific eutectic enthalpy of fusion of the binary mixture.

heights do not coincide very well because these widths, taken to be constant in the computed curves, depend on the initial composition w_2° in fact (see above). In contradistinction, the fusion peaks of the λ-transition of the remaining crystal within $T_E \leq T \leq T_m$ are in much better accord, although the experimental peaks are somewhat broadened out with respect to the calculated ones: that is, the computed DSC curves increase to a maximum of a relatively large extent which steeply, i.e. perpendicularly, falls to the amount of heat capacity of the melt, while the experimental curves gently (exponentially) approach this amount on passing their maximum.[10,29] This broadening called "smearing" is due to a limited heat transfer during a DSC treatment.[6] A simulation of "real" DSC curves with the attempt at taking this "smearing" into account will be the subject of the third part of this series.[5]

We devote the remainder of this section to a brief survey on the concentration dependence of the different contributions to the enthalpy of fusion. Figure 6 shows a sketch of the enthalpy of fusion, $\Delta\tilde{H}^{melt} = \int_{T_E}^{T_m} \tilde{c}_p^{melt}\, dT$ (curve 1a), the contribution of the base line, $\Delta\tilde{H}^{base} = \int_{T_E}^{T_m} \tilde{c}_p^{base}\, dT$ (curve 1b), and the total specific enthalpy of fusion, $\Delta\tilde{H} = \Delta\tilde{H}^{melt} + \Delta\tilde{H}^{base}$ (curve 1), each of which has been obtained by numerical integration of eqs 38b or 38c within the limits from T_E to T_m. In other words, the total enthalpy of fusion and $\Delta\tilde{H}^{base}$ are the areas below the DSC curve and the base line, respectively, while $\Delta\tilde{H}^{melt}$ corresponds to the area enclosed by these two curves. To complete the picture, the eutectic enthalpy of fusion (curve 2) has also been incorporated into Figure 6.

As can be seen from Figure 6, the specific enthalpy of fusion (curve 1a) and the eutectic enthalpy of fusion (curve 2) depend linearly on the initial composition w_2°. The proof of that for curve 2 ($\Delta\tilde{H}_E(w_2^\circ)$) has already been given above (see section 2.2), while the linearity of curve 1a becomes quite apparent, if eq 11a is inspected, which describes the enthalpy of state β at the eutectic temperature: after having passed the eutectic transition, the eutectic melt with composition w_2^E and the still remaining crystal with composition w_2'' are coexisting at temperature T_E (or rather at "$T_E + \delta T$"; see section 2.1). In turn, this crystal represented by the second term in eq 11a will be subjected to fusion in the following melting transition. As the pure solid component 2 (dodecane) is only present in the underlying binary system investigated (i.e. $w_2'' = 1$), the enthalpy of fusion must be given by

$$\Delta\tilde{H}^{melt} = \int_{T_E}^{T_m} \tilde{c}_P^{melt}\, dT = \frac{w_2^\circ - w_2^E}{1 - w_2^E}(\Delta\tilde{H}_{02} + \Delta\tilde{H}'_{mix}) \quad (45)$$

which is only applicable to binary systems whose components do not show any miscibility in the solid state. (It is worth noting that (1) the melt represented by the first term in eq 11a must not be considered here because this proportion (already molten) will be included in $\Delta\tilde{H}^{base}$; (2) even the most polar binary mixtures should depict the same behavior because enthalpies of mixing are negligible with respect to the enthalpies of fusion (differing by a factor of about 20); and (3) the enthalpy of fusion of systems, which are partially miscible in the solid state, is much more difficult to obtain owing to a further composition, w_2'' whose temperature dependence additionally requires to be taken into account). Equation 45 remains to be seen by integration of eq 38c with the reductions $w_2'' = 1$ and $\Delta\tilde{H}''_{mix} = 0$, which may be taken from the Appendix.

Contrary to curves 1a and 2, the contribution of the base line (curve 1b) and thus the total specific enthalpy of fusion (curve 1) do not show any linear behavior as a function of composition; both run through a maximum instead. This behavior proceeds from the same reason we have already discussed above: With increasing initial composition w_2°, the contribution of the base line is more and more governed by the heat capacities of the crystal, $\tilde{c}''_{P0i}$, compared with those of the liquid state, $\tilde{c}'_{P0i}$ (although $\tilde{c}''_{P0i} < \tilde{c}'_{P0i}$) because a constantly decreasing amount of the crystal has been fused at the eutectic point (corresponding to a decreasing quantity of the melt immediately after the eutectic transition). Regarding the numerical value of the specific heat capacity of the DSC curve at the end of the eutectic transition, it is thus the smaller, the greater w_2° is (see Figure 5). At the same time, the melting peak of the remaining crystal (λ-transition) is getting increasingly sharp and high (Figure 5) and the magnitude of the slope, concerning the temperature-dependent course of the base line, diminishes with a growing initial concentration w_2°.[5] Therefore the course of $\Delta\tilde{H}^{base}(w_2^\circ)$ in Figure 6 results from a contrary effect. On one hand there is a constantly decreasing $\tilde{c}_P$-value of the base line at T_E with growing w_2°. Simultaneously, the base line increases less and less such that $\Delta\tilde{H}^{base}(w_2^\circ)$ should be declining. On the other hand the range of fusion from T_E to T_m and hence $\Delta\tilde{H}^{base}$ should increase with w_2°. Both opposite effects eventually lead to the course of curve 1b depicted in Figure 6 that arrives at its maximum value at $w_2^\circ = 0.25$. Consequently, the total specific enthalpy (curve 1) evaluated of $\Delta\tilde{H}^{base}$ and $\Delta\tilde{H}^{melt}$ should also become maximum ($w_2^\circ = 0.94$).

6. Concluding Remarks

This paper is the first part of a series of papers that intend to correlate isobaric DSC curves with isobaric state diagrams quantitatively. It was devoted to calculating the "ideal" traces of DSC curves of binary mixtures from a known isobaric state diagram (here, "ideal" means being restricted to equilibrium conditions at any time). With this end in view, a binary model system consisting of two paraffins, *n*-hexane and *n*-dodecane, has been investigated by DSC with a scanning speed of 10 $K \cdot min^{-1}$.

Based on simple enthalpy and mass conservation considerations, some universal formulas have been derived that enable

one to compute the course of the specific heat capacity as a function of temperature while melting a binary sample. They may equally well be understood to be a generalized description of any other continuous phase transition of a binary mixture (λ-transition), such as evaporation, sublimation, and also mixing−demixing phenomena. This general treatment of a λ-transition has turned out to be advantageous insofar as the final expressions merely call for the knowledge of the respective equilibrium curves of the underlying phase diagram. In addition to that, they have, for convenience, been separated into thermodynamic properties of the pure components and mixing quantities in order to avoid using enthalpies of transfer instead which are not directly accessible by experiment. As invariant transitions of fusion quite frequently precede λ-transitions, we have also been dealing with the eutectic and the peritectic transition of fusion. The final relations resulting have turned out to be a quantitative approach to the so-called "Tammann's triangle" that allows us to establish the enthalpy of transition depending on the overall composition of the total system.

Owing to the fact that our binary model system is of the eutectic type, showing no miscibility in the solid state, some satisfactory reductions such as ruling out the enthalpies of mixing, were done. Due to the sparse literature data, the heat capacities of the pure liquid components were equated to standard heat capacities; those of the solid components have been estimated from experimental data. By the same token, the (unknown) temperature-dependence of the heat capacities of the pure compounds have not been taken into account.

Overall, the calculated ("ideal") traces of specific heat capacity versus temperature proved to be coincident for the most part with the experimental data. Drawing a comparison to the ideal traces, experimental DSC curves are slightly broadened ("smeared") due to heat transfer processes in the calorimeter during a DSC scan. We may thus take the exact thermodynamic expressions for binary $\tilde{c}_P(T)$ curves to serve, in first approximation, as a quantitative approach to λ-transitions of real DSC curves. An approach dealing with simulating "smeared" λ-curves will be presented in part 3 of this series.[5]

Inspection of the computed eutectic peaks has shown appreciable deviations with respect to their widths and heights. This is mainly due to the fact that the eutectic peaks—basically being discontinuous in thermodynamic terms—have conveniently been simulated by Gaussian curves with constant (identical) peak widths (or rather with identical standard deviations) despite being considerably affected by the initial composition and the location of the eutectic point, as we shall see in the next paper.[4]

Acknowledgment. The authors gratefully acknowlegde financial support from the Deutsche Forschungsgemeinschaft (DFG). Thanks are also given to Dr. Ralf Jüschke for giving us permission to use his program "WinReg 8.92" for graphical representations.

Appendix

We wish to prove that eq 45 results directly from integrating the expression

$$\tilde{c}_P^{\text{melt}} = \frac{1 - w_2^\circ}{(1 - w_2')^2}\left(\frac{\partial w_2'}{\partial T}\right)_P [\Delta\tilde{H}_{02} + \Delta\tilde{H}'_{\text{mix}}] \qquad \text{(A-1)}$$

which is equivalent to eq 38c simplified by the reductions $w_2'' = 1$ and $\Delta\tilde{H}''_{\text{mix}} = 0$. Let the temperature−concentration-dependence $T(w_2')$ be approached by the relationship

$$T = K_0 \ln[w_2' + K_1] + K_2 \qquad \text{(A-2)}$$

with K_0, K_1, and K_2 (with $|K_1| \ll 1$, and $K_2 \approx T_{\text{m},2}$) indicating the coefficients of this expression that is useful for an empirical description of experimentally determined $T(w_2')$-curves in spite of not being based on statistical thermodynamic relations. That is, although eq A-2 describes the experimental data in a very good approximation, it does *not* satisfy Raoult's limiting law. (In the interests of mathematical simplicitly we abstain from a rigorous treatment of the thermodynamic approach

$$T = T_{\text{m},2}\left\{1 - \frac{RT_{\text{m},2}}{\Delta\tilde{H}_{02}M_2}[\ln x_2' + A(1 - x_2')^2 + B(1 - x_2')^3]\right\}^{-1}$$

where A and B are understood to be empirical coefficients in the series expansion of the activity coefficient,[30,31] while $x_2' = w_2'/[w_2' + (1 - w_2')(M_2/M_1)]$ signifies the composition of the melt in the mole fraction scale of component 2 expressed by the corresponding mass fraction w_2' and the molecular masses M_1 and M_2 of components 1 and 2, leading to transcendental relations (which cannot be solved for w_2' without further approximations).) Incorporating eq A-2 in eq A-1 and taking $\Delta\tilde{H}_{02}$ and $\Delta\tilde{H}'_{\text{mix}}$ to be independent of temperature yield upon integration over T

$$\int_{T_{\text{E}}}^{T_{\text{m}}} \tilde{c}_P^{\text{melt}}\,\mathrm{d}T = (1 - w_2^\circ)(\Delta\tilde{H}_{02} + \Delta\tilde{H}'_{\text{mix}})\left[\left(1 + K_1 - \exp\left(\frac{T_{\text{m}} - K_2}{K_0}\right)\right)^{-1} - \left(1 + K_1 - \exp\left(\frac{T_{\text{E}} - K_2}{K_0}\right)\right)^{-1}\right] \qquad \text{(A-3)}$$

Due to the identities used (see eq A-2),

$$w_2^\circ = \exp\left(\frac{T_{\text{m}} - K_2}{K_0}\right) - K_1 \quad (T = T_{\text{m}} \Rightarrow w_2' = w_2^\circ) \qquad \text{(A-4)}$$

and

$$w_2^{\text{E}} = \exp\left(\frac{T_{\text{E}} - K_2}{K_0}\right) - K_1 \quad (T = T_{\text{E}} \Rightarrow w_2' = w_2^{\text{E}}) \qquad \text{(A-5)}$$

eq A-3 reproduces eq 45. If we allow $\Delta\tilde{H}_{02}$ and $\Delta\tilde{H}'_{\text{mix}}$ to alter with temperature, the bracketed term of eq A-1, which corresponds to the sum of the specific enthalpy of fusion of the pure component 2 and the specific enthalpy of mixing at the prevailing temperature T, needs to be replaced by the expression

$$\Delta\tilde{H}_{02}(T) + \Delta\tilde{H}'_{\text{mix}}(T) = \Delta\tilde{H}_{02}(T_{\text{m},2}) + \int_{T_{\text{m},2}}^{T}\left(\frac{\partial\Delta\tilde{H}_{02}}{\partial T}\right)_P \mathrm{d}T + \Delta\tilde{H}'_{\text{mix}}(T_{\text{m},2}) + \int_{T_{\text{m},2}}^{T}\left(\frac{\partial\tilde{H}'_{\text{mix}}}{\partial T}\right)_P \mathrm{d}T \qquad \text{(A-6)}$$

In this case, $\Delta\tilde{H}_{02}(T_{\text{m},2})$ and $\Delta\tilde{H}'_{\text{mix}}(T_{\text{m},2})$ are equivalent to the aforementioned quantities; however, each is related to the melting point $T_{\text{m},2}$ of component 2 (*n*-dodecane).

Glossary of Principal Symbols and Indices

English Letter Symbols

$\tilde{c}_P(T)$	Specific heat capacity of the DSC curve at temperature T
$\tilde{c}_P^{\text{base}}(T)$	Specific heat capacity of the base line of the DSC curve at temperature T
$\tilde{c}_P^{\text{melt}}(T)$	Specific heat capacity due to fusion at temperature T
$\tilde{c}_{P_{0i}}^{\delta}(T)$	Specific heat capacity of the pure component i in phase δ at temperature T
${}_\epsilon\tilde{H}_{T_{\text{E}}}$	Specific enthalpy of state ϵ at the eutectic temperature T_{E}

$\Delta\tilde{H}_E$ Specific enthalpy of fusion of the eutectic transition at temperature T_E (specific eutectic enthalpy of fusion) defined by eqs 1a or 1b

${}_\epsilon\tilde{H}_i^\delta(T,w_2^\delta)$ Partial specific enthalpy of component *i* in phase δ and state ϵ at the present composition w_2^δ and the prevailing temperature *T*

${}_\epsilon\tilde{H}_{0i}(T)$ Specific enthalpy of the pure component *i* in phase δ and state ϵ at the prevailing temperature *T*

$\Delta\tilde{H}_{0i}(T)$ Specific enthalpy of fusion of the pure component *i* at temperature *T*

$\Delta_\epsilon\tilde{H}^\delta_{mix}(T,w_2^\delta)$ Specific enthalpy of mixing of phase δ in the state ϵ at the present composition w_2^δ and the prevailing temperature *T*

i Substance index denoting component 1 or 2

Lq Liquidus curve representing the composition of the melt ***(I)*** as a function of temperature in the solid−liquid equilibria β and γ

m Total mass of the binary test sample

${}_\epsilon m^\delta$ Total mass of phase δ in the state ϵ

m_2 Mass of component 2

M_2 Molar mass of component 2

I, II, III Phase indices (superscripts) denoting the binary melt, the mixed crystal enriched by component 2, and the mixed crystal enriched by component 1

Sd Solidus curve representing the composition of the mixed crystal ***(II)*** or ***(III)*** as a function of temperature in the solid−liquid equilibria β and δ

Sv Solvus curve representing the composition of the mixed crystals ***(II)*** and ***(III)*** as a function of temperature in the solid−solid equilibrium α

T_I Start temperature of the DSC scan

T_{II} Final temperature of the DSC scan

T_E Melting temperature of the eutectic mixture (eutectic temperature)

T_m Melting temperature of the binary mixture

$T_{m,1}$, $T_{m,2}$ Melting temperatures of the pure components 1 and 2

$w_2'(T)$ Composition of the binary melt at temperature *T* ($T \neq T_E$)

$w_2''(T)$ Composition of the binary mixed crystal ***(II)*** at temperature *T*

$w_2'''(T)$ Composition of the binary mixed crystal ***(III)*** at temperature *T*

$w_2'(T) = w_2^E$ Composition of the binary eutectic mixture

w_2° Initial or overall composition of the test sample (mass fraction scale) given by m_2/m

Greek Letter Symbols

α State index (subscript) denoting the solid−solid equilibrium (coexistence of the two mixed crystals ***(II)*** and ***(III)***)

β State index (subscript) denoting the solid−liquid equilibrium (coexistence of the melt ***(I)*** and the mixed crystal ***(II)***)

γ State index (subscript) denoting the solid−liquid equilibrium (coexistence of the melt ***(I)*** and the mixed crystal ***(III)***)

δ Superscript comprising the phase indices (^{III}), (^{II}), and (^{E})

ϵ Subscript comprising the state indices α, β and γ

References and Notes

(1) Ehrenfest, P. *Proc. Kon. Akad. Wetenschr. Amsterdam* **1933**, *36*, 153.

(2) Tisza, L. *Generalized Thermodynamics*; M.I.T. Press: Cambridge, 1977; p 167ff.

(3) Kilian, H. G. *Koll. Z. Polym.* **1965**, *202*, 97.

(4) Müller, A.; Borchard, W. *J. Phys. Chem. B* **1997**, *101*, 4297.

(5) Müller, A.; Borchard, W. *J. Phys. Chem. B* **1997**, *101*, 4307.

(6) Müller, A.; Borchard, W. Part 4, in preparation.

(7) Müller, A.; Borchard, W. Part 5, in preparation.

(8) Hemminger, W.; Höhne, G. *Calorimetry−Fundamentals and Practice*; Verlag Chemie: Weinheim, 1984; p 67ff.

(9) Rosenberger, F. *Fundamentals of Crystal Growth I*; Springer: Berlin, 1979; p 81ff.

(10) O'Neill, M. J. *Anal. Chem.* **1964**, *36*, 1238.

(11) Roozeboom, H. W. B. *Die heterogenen Gleichgewichte vom Standpunkte der Phasenlehre*, Zweites Heft; Vieweg: Braunschweig, 1904; 1.-3. Teil.

(12) Kitaigorodsky, A. I. *Molecular Crystals and Molecules*; Academic Press: New York, 1973; p 105ff.

(13) Tammann, G. *Z. Anorg. Chem.* **1903**, *37*, 303. Tammann, G. *Lehrbuch der Heterogenen Gleichgewichte*; Vieweg: Braunschweig, 1924; p 124ff, 144ff.

(14) Haase, R. *Thermodynamik der Mischphasen*; Springer: Berlin, 1956; p 196ff.

(15) Haase, R. *Thermodynamik der Mischphasen*; Springer: Berlin, 1956; p 319ff.

(16) Tausend, A.; Wobig, D. *Z. Phys. Chem. N. F.* **1975**, *96*, 199.

(17) Borchard, W.; Luft, B.; Reutner, P. *Ber. Bunsen-Ges. Phys. Chem.* **1984**, *88*, 1010.

(18) Brennan, W. P.; Miller, B.; Whitwell, J. C. *Ind. Eng. Chem. Fundam.* **1969**, *8*, 314.

(19) Hemminger, W. F.; Cammenga, H. K. *Methoden der Thermischen Analyse*; Springer: Berlin, 1989; p 184ff.

(20) McNaughton, J. L.; Mortimer, C. T. *Registrierende Differential-Kalorimetrie*, offprint from "IRS; PC, Serie 2, 1975, Bd. 10", Perkin-Elmer & Co. GmbH: Überlingen.

(21) Hemminger, W. F.; Sarge, S. M. *J. Therm. Anal.* **1991**, *37*, 1455.

(22) Sarge, S. M.; Gmelin, E.; Höhne, G. W. H.; Cammenga, H. K.; Hemminger, W. F.; Eysel, W. *Thermochim. Acta* **1994**, *247*, 129.

(23) Arnauts, J.; Cooman, R. De; Vandeweerdt, P.; Koningsveld, R.; Berghmans, H. *Thermochim. Acta* **1994**, *238*, 1.

(24) Rehage, R.; Borchard, W. *The Physics of Glassy Polymers*; Haward, R. N., Ed.; Applied Science Publishers Ltd.: Barking, 1973.

(25) Kilian, H. G. *Progr. Colloid Polym. Sci.* **1986**, *72*, 60.

(26) Kilian, H. G. *Trends Polym. Sci.* **1993**, *3*, 571.

(27) Schmalzried, H. *Festkörperreaktionen: Chemie des festen Zustandes*; Verlag Chemie: Weinheim, 1971; p 55ff.

(28) Landolt-Börnstein, II./4, *Eigenschaften der Materie in ihren Aggregatzuständen: Kalorische Zustandsgrössen*; Springer: Berlin, 1961.

(29) Illers, K.-H. *Eur. Polym. J.* **1974**, *10*, 911.

(30) Haase, R. *Thermodynamik der Mischphasen*; Springer: Berlin, 1956; p 436ff.

(31) Kortüm, G.; Lachmann, H. *Einführung in die chemische Thermodynamik*; Verlag Chemie: Weinheim, 1981; p 198ff.